Lawrence Berkeley National Laboratory
LBL Publications

Title

Calculation of Properties of the Electron-Hole Liquid in Uniaxially Stressed Ge and Si

Permalink

https://escholarship.org/uc/item/28n100ds

Author

Kelso, S M

Publication Date

1981-12-01

Copyright Information

This work is made available under the terms of a Creative Commons Attribution License, available at https://creativecommons.org/licenses/by/4.0/

eScholarship.org Powered by the California Digital Library
University of California

LBL-13387
Preprint

Lawrence Berkeley Laboratory
UNIVERSITY OF CALIFORNIA

RECEIVED
BERKELEY LABORATORY
DOCUMENTS SECTION

Materials & Molecular Research Division

Submitted to Physical Review B

CALCULATION OF PROPERTIES OF THE ELECTRON-HOLE LIQUID IN UNIAXIALLY STRESSED Ge AND Si

S. M. Kelso

December 1981

TWO-WEEK LOAN COPY

This is a Library Circulating Copy which may be borrowed for two weeks. For a personal retention copy, call Tech. Info. Division, Ext. 6782

Prepared for the U.S. Department of Energy under Contract W-7405-ENG-48

LBL-13387

DISCLAIMER

This document was prepared as an account of work sponsored by the United States Government. While this document is believed to contain correct information, neither the United States Government nor any agency thereof, nor the Regents of the University of California, nor any of their employees, makes any warranty, express or implied, or assumes any legal responsibility for the accuracy, completeness, or usefulness of any information, apparatus, product, or process disclosed, or represents that its use would not infringe privately owned rights. Reference herein to any specific commercial product, process, or service by its trade name, trademark, manufacturer, or otherwise, does not necessarily constitute or imply its endorsement, recommendation, or favoring by the United States Government or any agency thereof, or the Regents of the University of California. The views and opinions of authors expressed herein do not necessarily state or reflect those of the United States Government or any agency thereof or the Regents of the University of California.

CALCULATION OF PROPERTIES OF THE ELECTRON-HOLE LIQUID IN UNIAXIALLY STRESSED Ge AND Si*

S. M. Kelso**

Materials and Molecular Research Division, Lawrence Berkeley Laboratory, and Department of Physics, University of California, Berkeley, CA 94720

and

Bell Laboratories, Murray Hill, NJ 07974

---

*Part of this work was supported by the Director, Office of Energy Research, Office of Basic Energy Sciences, Material Sciences Division of the U.S. Department of Energy under Contract No. W-7405-ENG-48.

**Present address: Xerox Palo Alto Research Center, Palo Alto, CA 94304

CALCULATION OF PROPERTIES OF THE ELECTRON-HOLE LIQUID IN UNIAXIALLY STRESSED Ge AND Si

*S. M. Kelso**

Physics Department, University of California and
Materials and Molecular Research Division,
Lawrence Berkeley Laboratory, Berkeley, CA 94720

and

Bell Laboratories, Murray Hill, N.J. 07974

We present a detailed theoretical study of the stress dependence of properties of the electron-hole liquid, both at zero and finite temperatures, in <111>-stressed Ge and <100>-stressed Si. These properties include the ground-state equilibrium density, pair energy, electron and hole Fermi energies, sign of the electron-hole drop charge, luminescence linewidth, and liquid compressibility. The results are compared at T=0 to the calculations of Kirczenow and Singwi and at T≈2K to the available data. We discuss the possibility of a phase transition associated with the depopulation of the upper electron valleys in Ge. We also discuss methods of extrapolating from finite to infinite stress. The importance of the nonparabolicity of the valence bands is emphasized throughout. We discuss ranges of validity for a low-temperature expansion of the free energy. Results are presented for the systematic low-temperature variation of the liquid density, Fermi energy, and chemical potential and for the critical temperature and density. These theoretical results are found to be in reasonably good agreement with available data. Finally, we discuss scaling relations for combinations of electron-hole liquid properties.

---

* Present address: Xerox Palo Alto Research Center, Palo Alto, CA 94304.

I. Introduction

The first theories of the electron-hole liquid[1] (EHL) in semiconductors were concerned with predicting and understanding the properties of the EHL for systems in which it had already been observed experimentally, i.e., unstressed Ge and Si.[2–4] It is well known that the band structures of Ge and Si simplify under infinite uniaxial compression: for <111>-stressed Ge only a single conduction band minimum remains occupied, while for <100>-stressed Si two conduction band minima remain occupied; in both cases the single populated valence band becomes ellipsoidal. Because of these simplifications, the infinite-stress limit was also considered theoretically.[2,3] These calculations predicted that the EHL would be unbound or just barely bound with respect to free excitons in Ge. However, the more sophisticated calculations of Vashishta et al.[5] indicated that the EHL should be observable in the infinite-stress limit. All the calculations predicted that the electron-hole pair density would be considerably reduced compared to that of unstressed crystals. Vashishta et al.[6] also performed a calculation for an ideal intermediate-stress case in which the electrons were treated as for infinite stress and the holes as for zero stress; the results were intermediate between the zero- and infinite-stress theories. In addition, the effects of finite temperature on EHL properties and the critical point were estimated for zero and infinite stress, using an expansion valid at low T.[7–9]

In the meantime, several experiments[10–12] were performed to study the EHL in Ge and Si stressed along the three principal crystallographic directions. In these early experiments a stable liquid phase was observed under moderate stresses. Although the luminescence spectra shifted with stress, they were not analyzed in enough detail to determine the properties of the EHL. Experiments performed on inhomogeneously stressed Ge showed that at moderate stresses the electron-hole pair density is reduced from its value in unstressed Ge.[13,14] More recently, systematic experiments have been performed on Ge under <111> uniaxial stress[15–19] and on Si under <100> stress[20] to study the stress dependence of EHL properties.

Since experiments cannot be performed at infinite stress or zero temperature, it is clearly

desirable to have a finite-stress, finite-temperature theory. A first attempt to predict the systematic variation of the ground state (T=0K) properties of the EHL in <111>-stressed Ge was made by Markiewicz and Kelso.[21] In that paper, the stress dependence of the holes was taken into account but the electrons were treated as for infinite stress, so the results are valid only for the intermediate- to high-stress range. Liu et al.[22,23] performed a calculation for two values of the stress, for both Ge and Si, and included a low-T expansion to estimate the critical point. Kirczenow and Singwi have considered the systematic stress dependence of some EHL properties in Ge[24] and Si,[25] restricted to T=0.

In this paper we present detailed calculations[26,27] of the properties of the electron-hole liquid as a function of compressive <111> stress in Ge and <100> stress in Si, both at T=0 and finite temperature. We include the full stress dependence of the conduction and valence bands in the kinetic energy, except that the split-off valence band is ignored. Energy- and stress-dependent hole masses, introduced previously,[14,21,28] are used to describe the nonparabolicity of the valence bands. We initially consider several models for the exchange-correlation energy; two include separate stress and density dependences. We compare the exchange-correlation energies directly, as well as results for the EHL ground-state density and energy. Two models are selected for further calculations and for comparison with experiment. We believe that uncertainty in the mathematical representation of the correlation energies of Vashishta et al. can result in model-dependent predictions. Consequently, one of the models selected for our detailed calculations uses a simple empirical correlation energy. Both models are different from those considered by Kirczenow and Singwi.[24,25]

Results are presented for several properties of the EHL at T=2K to facilitate comparison with experiment. In addition to the density, we discuss the electron and hole Fermi energies, the sign of the charge on electron-hole drops (EHD), and the binding energy, ϕ, of the EHL with respect to free excitons. While there is overall qualitative agreement between theory and experiment, some quantitative differences are discussed.

It is convenient to introduce two critical values of stress. When the stress-induced splitting of the conduction bands, E^e_{spl}, is equal to the electron Fermi energy, E^e_F, the upper electron valleys are depopulated (at T=0). Thus a critical stress, σ_e, is determined by the condition $E^e_{spl} = E^e_F$. Similarly, a critical stress, σ_h, associated with the emptying of one valence band is defined by the condition $E^h_{spl} = E^h_F$.

In agreement with Kirczenow and Singwi,[24,25] we find a rapid decrease in the electron-hole pair density associated with the emptying of the upper conduction bands at σ_e. For Ge at T=0, we discuss the possibility of two different types of EHL, with a phase transition as a function of stress. Our model-dependent results indicate a critical dependence on details of the exchange-correlation energy, such as curvature with respect to density, which are not well known. We show by explicit calculation that the change in the number of occupied conduction bands is an important factor in the possibility of a discontinuous change in the equilibrium density at σ_e; thus the unambiguously more gradual density change predicted for Si is understood.

We predict significant changes in all EHL properties for stresses beyond σ_h. Since no further changes take place in the number of occupied bands, the high-stress variation of EHL properties arises solely from the residual nonparabolicity of the valence band, which remains important even after the bands are well split in energy. Because these variations continue well past σ_h, we discuss procedures for extrapolating finite-stress data to the infinite-stress limit.

For finite temperatures, both low-T and high-T limits are considered. At sufficiently low temperatures we find that the usual expansion for the kinetic energy of a degenerate Fermi system is valid, except at stresses very near σ_e and σ_h. We discuss the systematic low-T variation of EHL properties, using derivatives of the ground-state free energy versus density. Near the critical point, however, we find that the expansion is no longer valid at any stress. Thus we calculate the kinetic energy exactly at all finite temperatures. Our theoretical results are compared with available data. In addition, we consider scaling relations of certain combinations of EHL properties as the band structure changes with stress.

The paper is divided into several sections. The calculation of the free energy of electrons and holes at arbitrary stress and temperature is described in Section II. Results for ground-state EHL properties are presented in Section III. Finally, results for finite temperatures are presented in Section IV.

II. Formalism: The Free Energy at Arbitrary Stress and Temperature

We begin with some basic thermodynamic definitions for a neutral plasma of electrons and holes. The total free energy F is a function of the number of electron-hole pairs N, volume V, and temperature T (assumed here to be the lattice temperature). It is convenient to work with the free energy per pair $f \equiv F/N$ and the pair density $n \equiv N/V$, and to consider variations of f with n. We note the following definitions and simplifications:

$$F \equiv U - TS = N\mu - PV \tag{1a}$$

where

$$P \equiv -\left(\frac{\partial F}{\partial V}\right)_{T,N} = n^2\left(\frac{\partial f}{\partial n}\right)_{T,N} \tag{1b}$$

is the pressure and

$$\mu \equiv \left(\frac{\partial F}{\partial N}\right)_{T,V} = f + n\left(\frac{\partial f}{\partial n}\right)_{T,V} \tag{1c}$$

is the chemical potential. The second equality in Eq. (1a) comes from the definition of the grand potential:

$$\Omega \equiv -PV = U - TS - N\mu \,. \tag{1d}$$

For the electron-hole liquid, the free energy is separated into kinetic and exchange-correlation energy contributions,

$$F = F_{kin} + F_{excor} \,, \tag{2}$$

which are treated in the next two subsections.

A. Kinetic Energy

The kinetic energy term is just the free energy for a gas of free Fermi particles. The grand potential for carriers in a band with a density of states D(E) is given by

$$\Omega \equiv -kT\int_0^\infty D(E)\ln\left[1+e^{(E_F-E)/kT}\right]\,dE \tag{3a}$$

$$= -\int_0^\infty \left[\int_0^E D(u)du\right]\left[1+e^{(E-E_F)/kT}\right]^{-1} dE\,. \tag{3b}$$

The Fermi energy, E_F, is determined by the relation

$$N \equiv -\left[\frac{\partial\Omega}{\partial E_F}\right]_{T,V} = \int_0^\infty D(E)\left[1+e^{(E-E_F)/kT}\right]^{-1} dE \tag{4}$$

and depends on temperature. The free energy is obtained from Eqs. (1a), (1d), and (3b):

$$F = NE_F - \int_0^\infty \left[\int_0^E D(u)du\right]\left[1+e^{(E-E_F)/kT}\right]^{-1} dE\,. \tag{5}$$

Information about the band structure is contained in the density of states. As has been noted previously,[28] it is convenient to write

$$D(E) = \frac{\sqrt{2}V}{\pi^2\hbar^3}\, m_{dloc}^{3/2}(E)\, E^{1/2}\,, \tag{6a}$$

where $m_{dloc}(E)$ is a local density-of-states mass given by

$$m_{dloc}^{3/2}(E) \equiv \frac{\hbar^3}{4\sqrt{2}\pi E^{1/2}} \int k^2 \frac{dk}{dE}\, d\Omega\,. \tag{6b}$$

The integration is performed over solid angle on the k-space surface with energy E. This mass depends on energy only if the band is nonparabolic, as is the case for the valence bands in germanium or silicon at finite stress. Results for <111>-stressed Ge and <100>-stressed Si are given in Ref. 28 (see Figs. 1c and 2a). The conduction band is assumed to be parabolic, with the same energy-independent density-of-states mass at all stresses.

In stressed Ge or Si the conduction and valence bands are both split by the stress, with only the band(s) lowest in energy remaining populated at high stress. Suppose that a set of $\nu_1+\nu_2$ bands, degenerate at zero stress, becomes split by an energy E_{spl}, with ν_1 bands below the other ν_2 bands. For example, in <111>-stressed Ge, $\nu_1 = 1$ and $\nu_2 = 3$ for electrons while $\nu_1 = \nu_2 = 1$ for holes. In this case the density of states becomes

$$D(E) = \frac{\sqrt{2}V}{\pi^2\hbar^3}\left\{\nu_1 m_1^{3/2}(E)E^{1/2} + \nu_2 m_2^{3/2}(E)(E-E_{spl})^{1/2}\right\}, \tag{7}$$

where $m_1(E)$ and $m_2(E)$ are the local density-of-states masses for the two sets of bands and E is measured from the bottom of the band for the lower set. It is understood that $m_2(E) = 0$ for $E<E_{spl}$. This form for the density of states should be used in Eqs. (4) and (5). We use the same Fermi level for both subsets, indicating that all the carriers are in thermal equilibrium with each other. This corresponds to the equilibrium limit of Kirczenow and Singwi.[24]

Equations (4)-(6) may be used separately for electrons and for holes, with

$$N_e = N_h = N \text{ and } F_{kin} = F^e_{kin} + F^h_{kin}\,. \tag{8}$$

Note that, for a particular temperature and stress, f^e_{kin}, f^h_{kin}, and $n_e = n_h$ depend only on the relevant Fermi energy E^e_F or E^h_F. Thus, for fixed stress, f is a function only of n and T:

$$\left(\frac{\partial f}{\partial n}\right)_{T,N} = \left(\frac{\partial f}{\partial n}\right)_{T,V} = \left(\frac{\partial f}{\partial n}\right)_{T}. \tag{9}$$

The procedure for calculating the kinetic energy f_{kin} was as follows: (1) a hole Fermi energy E^h_F was chosen; (2) the density was computed using Eq. (4) for holes; (3) the electron Fermi energy E^e_F was obtained by inverting Eq. (4) for electrons; (4) f^e_{kin} and f^h_{kin} were computed using Eq. (5). We usually wanted to find a minimum in f(n) or the disappearance of a minimum in μ(n). These minima were often very shallow: for example, in order to determine the equilibrium density at T=0 to within 1% it was necessary to calculate f(n) to a precision of 1 part in 10^6. Of course, the band structure parameters are not known this well, but it was desirable to reduce the mathematical uncertainties.

At finite temperature the kinetic energy was computed exactly, rather than using the T^2 expansion employed by other authors[7,8,23] (see discussion in Sec. IVB). The integrals in Eqs. (4) and (5) are (modified) Fermi-Dirac integrals for the electrons (holes). Since they cannot be evaluated analytically at finite temperature, they must be computed numerically. Some care must be taken to ensure that the results vary sufficiently smoothly with hole Fermi energy. For example, it was necessary to iterate the step (3) inversion to convergence.

The local density-of-states hole masses given by Eq. (6b) and by the valence band structure of Ge and Si were calculated numerically as a function of reduced energy $E' \equiv E/\sigma$ (see Ref. 28). The results for the two bands were fit to simple analytic functions over several ranges of E', matching the functions and their first derivatives at the crossover points between the ranges. This procedure, in conjunction with the numerical integration at finite T, was found to be satisfactory.

The zero-temperature calculation is much simpler. The integrals in Eqs. (4) and (5) are trivial for electrons. For holes, the integrals can be performed analytically by directly integrating the formulas for the local masses.

B. Exchange-Correlation Energy

The exchange-correlation energy is usually separated into two terms:

$$F_{excor} = F_{ex} + F_{corr} . \tag{10}$$

As in all other calculations to date, we suppose that the exchange-correlation energy is independent of temperature[9] and use results for T=0. A detailed first-principles calculation, including the effects of finite stress on the band structure, would be extremely difficult and has not been attempted. However, such a calculation is not really necessary: the exchange-correlation energy appears to be largely independent of such band structure details as masses, anisotropies, and degeneracies, as long as both the exchange and correlation energies are calculated using the *same* details.[29,30] One reason for this is that the separate dependences of the

exchange and correlation energies on the band structure, which can be substantial, tend to cancel in the sum.[31] This cancellation has been exploited in other zero-temperature calculations.[21,24,25,30] In addition, Vashishta has suggested[32] that the correlation energy should depend only weakly on the (hole) mass. Here we consider both of these ideas.

For zero or infinite stress the exchange energy per electron-hole pair is given by

$$f_{ex} = -\frac{3e^2}{4\pi\kappa}(3\pi^2 n)^{1/3}\left[\frac{\phi(\rho_e)}{\nu_e^{1/3}} + \psi(\rho_h)\right], \tag{11}$$

where ν_e is the number of electron valleys and $\rho = m_t/m_l$ is the electron or hole anisotropy parameter. Values for $\phi(\rho_e)$ and $\psi(\rho_h)$ are listed in Table I, along with other parameters used in the calculations.

We considered six models for the exchange-correlation energy, summarized in Table II. The first three models were used in our preliminary calculations for Ge.[21] The scheme used for Models 1 and 2 (infinite-stress electrons, zero-stress holes) is intended[6,33] to most closely represent an intermediate stress near σ_c, although it does not correspond exactly to any value of stress. The Model 1 correlation energy uses the results of a detailed numerical calculation[34] in a fully self-consistent (FSC) approximation[4,5,7] including multiple scattering and band anisotropy. The results were fit to a polynomial in the interparticle spacing r_s for higher densities and matched to a Wigner form for lower densities.[35] In Model 2, this detailed calculation is replaced by a simple empirical correlation energy, taken to be a sum of Wigner-type contributions from the electrons and holes:[36]

$$f_{corr} = -\frac{c}{n^{-1/3} + a/m_{oe}} - \frac{c}{n^{-1/3} + a/m_h}, \tag{12}$$

where m_{oe} is the electron optical mass and m_h is a hole mass, here the infinite-stress optical mass. The constants a and c are chosen to match the value and first derivative of Eq. (12) to the Model 1 correlation energy at the equilibrium density for the "ideal" system (infinite-stress electrons, zero-stress holes in the kinetic energy). Values for a, c, and the masses are given in

Table I.

Models 3 and 4 represent attempts to determine the effect of a dependence of the correlation energy on the hole mass, which varies with density and stress.[28] Both models are similar to Model 2: the correlation energy has the form of Eq. (12) and is matched to Model 1 in the same way as Model 2. In Model 3, m_h is the optical mass averaged over the longitudinal and transverse components of the two hole bands (see the curves labelled m_{opt} in Figs. 3c and 4a of Ref. 28). In Model 4 we use the integrated density-of-states mass (see the curves m_{d1}^{int} and m_{d3}^{int} in Figs. 1c and 2a of Ref. 28) averaged over the two hole bands.

Models 5 and 6 were chosen to illustrate two extreme cases in which both the exchange and correlation energies are calculated using the same band structure details. Model 5 uses an exchange-correlation energy appropriate for zero stress, while Model 6 uses one appropriate for infinite stress. The correlation energies are the FSC results of Kalia and Vashishta,[33] and are very similar to models considered by Kirczenow and Singwi.[24,25,30]

Variations among the exchange-correlation energies are investigated conveniently by considering ratios of different models. Models 1, 5, and 6 are compared to Model 2 in Figs. 1 and 2 for Ge and Si, respectively. In these models, the density dependence is independent of stress. Model 2 was selected as the normalization model because it uses a simpler form for the correlation energy. The maximum spread between these models is only about 15% for Ge and 10% for Si over a range of two orders of magnitude in density. Several of the FSC models appear to exhibit small oscillations in the figures. It should be emphasized that these oscillations, *relative* to Model 2, do not occur in the individual exchange-correlation energies. They are artifacts of the fitting polynomials. It is clear, however, that the curvature of the exchange-correlation energy may not be well represented by certain models. This will be important for the calculation of the critical point and is discussed further, along with the dashed curves, in Section IVB.

III. Results: Ground-State Properties

In this section we present results for the ground-state properties of the electron-hole liquid in <111>-stressed Ge and <100>-stressed Si. First we compare results for the six models with each other and with other calculations. Next we discuss a possible phase transition associated with the emptying of the upper electron valleys in Ge. Finally, we compare the results at T=2K with the available data and give guidelines for extrapolating to the infinite-stress limit.

A. Comparison of Models

The ground state of the EHL occurs at the density for which the free energy per electron-hole pair is a minimum at T=0K. It is convenient to have the computer search for the associated zero in the pressure, as in Eq. (1b). The ground state densities n_o are shown as a function of compressive stress σ in Figs. 3 and 4 for Ge and Si, respectively. According to convention, compressive stresses are negative and are expressed in kgf/mm^2, where 1 kgf = 9.80665 Newton. In both figures, part (a) shows the results for the models based on FSC correlation energies, while part (b) shows the results for the models which use Wigner-type correlation energies. Arrows indicate the values which should be most nearly correct at zero and infinite stress (Models 5 and 6, respectively).

As expected, all the models show the same general trends with stress: (1) A fairly rapid decrease in density occurs near the critical stress σ_e, where $E_F^e = E_{spl}^e$ and the upper electron valleys become depopulated. The density change is larger for Ge due to the greater change in the number of occupied valleys. (2) The density remains nearly constant between σ_e and σ_h, where $E_F^h = E_{spl}^h$ and the lower hole band becomes depopulated. (3) A slight kink in n_o occurs at the stress σ_h, followed by (4) a further gradual decrease in density which is still apparent at stresses much greater than σ_h. As shown below, $-\sigma_h \approx$ 6 kgf/mm^2 in <111>-stressed Ge and $-\sigma_h \approx$ 37 kgf/mm^2 in <100>-stressed Si. Indeed, the equilibrium density changes by over a factor of 2 in Si and by approximately a factor of 4 in Ge after σ_h. In Models 1, 2, 5,

and 6 this stress dependence comes entirely from the hole kinetic energy contribution and arises from the residual nonparabolicity of the occupied ($|M_J|=1/2$) valence band. Thus the valence bands do not decouple until they are split quite far apart in energy[21,22,27] (see also Section IIIC).

The results for Model 3 show an oscillation in the equilibrium density associated with a local maximum in the hole optical mass used in the correlation energy. Model 4 does not exhibit an oscillation, since the hole density-of-states mass changes monotonically with stress. The kink associated with σ_h is more pronounced for Si because the hole mass is changing more quickly. Models 3 and 4 predict the lowest high-stress densities due to the significant change in the hole mass with stress.

While Models 2, 3, and 4 are very similar at low stresses and show greater differences at high stresses, the opposite is true for Models 1, 5, and 6. The spread among the results for the latter models is nearly 50% at zero stress but only ~10% at infinite stress.

Our results may be compared to other calculations. For Ge, Model 6 is virtually identical to one model used by Kirczenow and Singwi[24] and is similar to the model used by Liu et al.;[22,23] the results are correspondingly similar. The second model used by Kirczenow and Singwi does not correspond to any of the present models. Their results are most similar to Model 1, except that their equilibrium density falls off more rapidly at high stresses, somewhat like Model 4.

Similar comments apply to a comparison with other calculations[22,23,25] for Si. However, we note that we have used deformation potentials for Si which are different from those implied by Kirczenow and Singwi.[25] As shown in Table I, the deformation potentials used here yielded a ratio of conduction to valence band splitting $E^e_{spl}/E^h_{spl} = 3.2$, compared to a ratio of 1.81 used by Kirczenow and Singwi.[37] For Ge we used a ratio $E^e_{spl}/E^h_{spl} = 2.9$, in agreement with the ratio used by Kirczenow and Singwi.[24]

The ground-state energy per pair, f_G, is shown for all six models in Figs. 5 and 6. A rather sudden change in slope occurs at the stress σ_e. The EHL is bound with respect to free excitons

if $|f_G|$ is greater than the exciton binding energy E_x. For infinite stress E_x is the excitonic Rydberg,[38] which is 2.65 meV for Ge and 12.85 meV for Si. These values are shown as dashed lines in Figs. 5 and 6. For zero and intermediate stresses the exciton structure is complicated due to the valence-band degeneracy and the conduction-band anisotropy.[39] Experimental values for the binding energy of the lowest zero-stress exciton state are 4.15 meV for Ge[40] and 14.7 meV for Si.[41] Independent of the details of the variation of E_x at intermediate stress, which has been neither measured nor calculated, the binding energy of the liquid with respect to free excitons is expected to decrease rather rapidly with stress at low stresses. This effect has been observed both in Ge[42] and in Si.[20,43] Comparing to the dashed lines in the figures, our calculations predict a bound liquid state at all stresses, with the exception of Models 3 and 4 above $-\sigma \approx 23$ and 13 kgf/mm^2, respectively, in Ge and Model 4 above $-\sigma \approx 44$ kgf/mm^2 in Si.

For further calculations it is unnecessary to consider so many models. We note that a bound liquid state has been observed in Si (Ge) at high stresses where Model(s 3 and) 4 does (do) not predict binding (see Section IIIC). In addition, since the hole mass variations in Models 3 and 4 were omitted from the exchange energy, both models probably overestimate the effect of the changes in the valence band on the exchange-correlation energy. These models will not be discussed further. Among the models based on FSC correlation energies, we select Model 1 as a reasonable average. The Wigner-based Model 2 provides a useful complement since the correlation energies agree in value and slope at one point but have different curvatures and density dependences. Thus Models 1 and 2 will be compared in detail.

Numerical results for several ground-state properties of the EHL are listed in Table III for selected stress values for Models 1 and 2. In addition the Model 5 zero-stress and Model 6 infinite-stress results are listed, along with experimental values for zero stress.[1] The first stress is slightly greater than $-\sigma_e$, so that the upper electron valleys are depopulated. Similarly, the second stress is slightly greater than $-\sigma_h$, so that only one valence band is populated. The final stress is a few times $-\sigma_h$ and illustrates that further changes occur before the high-stress limit

is attained.

B. Possible Phase Transition in Ge Near σ_c

We noted in the previous section that a rapid change in the equilibrium density occurs just below the critical stress σ_c. Our detailed calculations for Models 1, 5 and 6 in Ge showed[27] that the pair free energy has two minima as a function of density in a very narrow range of stresses ($\Delta\sigma \lesssim 0.1$ kgf/mm^2) around σ_c. At T=0, the true ground state of the system is associated with the minimum having the lowest energy f_G. As the stress changes the relative energies of the two minima change. Thus the calculations predict a discontinuous decrease in n_o (i.e., a phase transition) as the stress increases. This is indicated in Fig. 3a by dashed lines. The possibility of such a discontinuous change in density was noted independently by Kirczenow and Singwi[24] but seems less clear for the equilibrium limit in their calculations.

The prediction of a double minimum in the free energy for Ge is not model independent: Models 2, 3 and 4 predict a *rapid but continuous* change in n_o (see Fig. 3b). Andryushin et al.[44] used a model in which the valence band changes were ignored and which employed a Combescot-Nozieres form[2] of the correlation energy; they found no phase separation. On the other hand, Kastal'skii's Hartree-Fock calculation (no correlation energy) does predict a double minimum.[45] Corresponding calculations for <100>-stressed Si[25,27,44] predict that the double minimum does not occur for that system.

We examined the free energy curves for Ge in some detail[27] and found that the height of the energy barrier between the two minima was very small, less than $\approx$0.004 meV or 0.05K. Whether two minima occur, as for example in Model 1, or only one minimum, as for example in Model 2, depends very sensitively on the details of the density dependence of the correlation energy in the range $n \approx (0.6\text{-}1.5) \times 10^{17}$cm^{-3}. The ratio of the exchange-correlation energies for Models 1 and 2 varies between 1.000 and only 1.005 in this range. It is difficult to distinguish between the mathematical representations on a first-principles basis.

Whether or not a *discontinuous* change occurs in the density it is clear from Fig. 3 that n_o should change by approximately a factor of two in a very narrow range of stress, perhaps a few tenths of a kgf/mm^2. Some recent data,[19] discussed in the next subsection, appear to agree with this prediction.

For the case of <100>-stressed Si, the density decrease in Fig. 4 associated with the depopulation of the upper electron valleys is smaller and more gradual than for Ge. The change in the number of populated conduction bands is smaller in Si than in Ge. To investigate the effect of the relative change in the number of occupied conduction bands, a series of artificial models was constructed. The models were similar to Model 1 for <111>-stressed Ge, with the number ν_2 of upper electron valleys a parameter. The ground-state equilibrium densities for several models with ν_2 ranging from 1 to 9 are shown in Fig. 7. The curve labelled $\nu_2 = 3$ thus corresponds to Ge, while the curve labelled $\nu_2 = 2$ corresponds (qualitatively) to Si, since the electron valley degeneracy changes by the same factor of 3. It is clear that a large relative change in the conduction band degeneracy, which is accompanied by a rapid variation in the electron kinetic energy, tends to favor the formation of a double minimum.

It would be very interesting if nature provided a real system with a large change in a band degeneracy. In the alloy $Ge_{1-x}Si_x$, with $x \approx 0.15$-0.20, the four Ge-like <111> conduction-band minima and the six Si-like <100> minima are degenerate.[46] With the application of <111> uniaxial stress the <100> valleys would remain degenerate while the <111> valleys would become stress-split. Thus the number of EHL-occupied conduction bands would change from 10 to 7 to 1 for increasing <111> stress. Other indirect semiconductor alloys in which the <111>- and <100>-associated minima become degenerate include the III-V pseudobinaries $In_{1-x}Ga_xP$ ($x \approx 0.77$)[47] and $Al_xGa_{1-x}Sb$ ($x \approx 0.56$)[48]. Although the EHL has not yet been observed in the latter materials, an experimental study of such a system would provide valuable insight into the nature of this proposed phase transition.

C. Comparison with Experiment: The Approach to the Infinite-Stress Limit

The results of our calculations using Models 1 and 2 are compared with experiment in this section. Because experiments are typically performed with the sample immersed in pumped liquid Helium, the calculations have been redone for T=2K. The procedure for the finite-temperature calculation of the free energy was described in Section II. At T=2K the gas pressure outside the EHL is sufficiently low that the equilibrium density is given very accurately by the free-energy minimum.

We consider first the results for <111>-stressed Ge. Figure 8 shows the theoretical equilibrium density along with several sets of data obtained at temperatures in the range T = 1.8-2.1K. Note that Model 1 predicts a discontinuous density change at σ_e even at T=2K, but we find that the energy barrier between the minima is even lower than at T=0. The experimental densities were obtained by fitting luminescence spectra from the EHL in uniaxially stressed Ge[16–18] or from the strain-confined EHL[14] or by fitting plasma resonance lineshapes for uniaxially stressed samples.[19] In all cases the lineshape analyses were performed using the appropriate energy- and stress-dependent hole masses.[27,28] Overall, theory and experiment are in reasonable agreement. The density decrease associated with the emptying of the upper electron valleys is not as pronounced in the data as in the theory. However, a decrease of a factor of two in density has been observed within a very narrow stress range, less than half a kgf/mm^2, by Zarate and Timusk.[19]

While the data of Zarate and Timusk agree very nicely with Model 2, the data of Feldman et al.[16] and of Chou and Wong[17] decrease more rapidly at higher stresses than the predictions of either model. Although care was taken to assure stress uniformity in the experiments, we note that residual nonuniformity will result in broader spectra and higher deduced densities. Thus, if the stress calibrations are accurate and if comparable lineshape analyses are performed, the narrower spectrum and lower density should be more nearly correct.

The EHL work function ϕ has been measured spectroscopically from EHL and exciton luminescence spectra at two stresses. Furneaux et al.[14,49] found $\phi \approx 1$ meV at $-\sigma \approx$

6 kgf/mm^2. A theoretical upper limit to ϕ is obtained using the infinite-stress E_x; we find $\phi \lesssim 1.15$ meV for both models. In addition, Feldman et al.[15] measured $\phi = 0.65 \pm 0.07$ meV at $-\sigma = 13$ kgf/mm^2, compared to 0.82 meV for Model 1 and 0.77 meV for Model 2. The agreement is quite satisfactory.

The electron and hole Fermi energies, E_F^e and E_F^h, are shown in Fig. 9. The dashed lines are the conduction and valence band splittings, E_{spl}^e and E_{spl}^h. The critical stresses, determined by the relations $E_F = E_{spl}$, are

$$\left.\begin{aligned} -\sigma_e &\approx 2.5 \text{ kgf/mm}^2 \\ -\sigma_h &\approx 6 \text{ kgf/mm}^2 \end{aligned}\right\} \text{Ge, T=2K, <111>stress} \qquad (13)$$

for both models. At low stresses, the electron Fermi energy is forced to increase as the upper electron valleys begin to depopulate; the hole Fermi energy decreases gradually as the density decreases. The changes in the electron kinetic energy become increasingly important near σ_e, and the density and both Fermi energies decrease rapidly. Above σ_e, E_F^e decreases smoothly, tracking the density, since there are no further changes in the conduction band structure. The changes in the hole Fermi energy between σ_e and σ_h reflect the changes in the population of the $|M_J|=3/2$ valence band and in the hole mass. Above σ_h the decrease in E_F^h and n is due to the decrease in the density-of-states hole mass.[27]

Several of the general features of the theoretical curves in Fig. 9 are observed experimentally. The data of Thomas and Pokrovskii[18] and of Chou and Wong[17] are shown as circles and triangles, respectively, where the solid (open) symbols indicate E_F^e (E_F^h). The electron Fermi energy increases at low stresses, as predicted. However, the sharp decrease in both Fermi energies which should denote σ_e is not observed. Both theoretically and experimentally $E_F^h > E_F^e$ below σ_e and above σ_h, while the reverse is true between σ_e and σ_h. The decrease in the experimental Fermi energies relative to theory at higher stresses parallels the densities in Fig. 8.

The Fermi energies can be used to predict the electric charge on electron-hole drops. An EHD can become charged if the electron and hole chemical potentials differ. Because the electron and hole contributions to the exchange-correlation energy are nearly equal,[50] the sign of the chemical potential difference is given by the difference in Fermi energies. If $E_F^h > E_F^e$ then holes are less tightly bound to the EHD than electrons; holes evaporate, leaving the drop negatively charged. From Fig. 9 we find that EHD should be negatively charged in the stress ranges below σ_e and above σ_h, approximately, and positively charged in the intermediate range. These predictions are in agreement with the detailed calculations of Kalia and Vashishta[33] for three ideal cases. Pokrovskii and Svistunova[51] found experimentally that EHD are negatively charged in unstressed Ge, become positively charged around $-\sigma \approx 2$ kgf/mm^2, and remain positively charged at least up to $-\sigma \approx 9$ kgf/mm^2. The last result is difficult to interpret since the luminescence spectra obtained by the same authors[52] indicate that E_F^h has become larger than E_F^e. Further experiments at higher stresses would help resolve this discrepancy. The experimental results for lower stresses, however, are in excellent agreement with the predictions.

We turn now to a comparison with experimental results for <100>-stressed Si. Figure 10 shows curves for Models 1 and 2 of the full-width-at-half-maximum linewidth, ΔE, of luminescence spectra computed for the T=2K equilibrium densities. The procedure for calculating luminescence spectra at finite stress has been discussed previously.[28] We show calculations of ΔE to facilitate comparison with raw data independent of fitting procedures. The theoretical curves show a rapid decrease in the luminescence linewidth associated with the emptying of the upper electron valleys and a much smaller decrease associated with the emptying of the $|M_J|=3/2$ hole band. The figure also shows several sets of experimental points.[20,53–57] With the exception of the points from Wagner and Sauer[55] the data are in excellent agreement with each other. This is notable because the spectra have been analyzed using different procedures, in some cases[54,55,57] incorrect ones, resulting in different deduced densities for the same value of stress.[28]

Although the experimental linewidth decreases with stress, the details of the decrease differ markedly from theory. In particular, the sharp decrease associated with the critical stress σ_c is not observed experimentally. We note that there should be no ambiguity associated with the conduction band deformation potential, since several measurements are in good agreement.[58] However, the discrepancy between experiment and theory occurs in a stress range where the equilibrium limit used in the calculation may not be appropriate: intervalley scattering is inhibited because E^e_{spl} is too small to allow the participation of TA phonons.[55] If the experiment samples non-equilibrium-limit conditions then the average observed density and linewidth will be larger than for the equilibrium limit.[25] More efficient intervalley thermalization takes place above $\sim$25 kgf/mm^2 (Ref. 55). This provides a qualitative understanding for the difference between theory and experiment in the intermediate stress range.

The luminescence spectra obtained by Gourley and Wolfe were analyzed using energy- and stress-dependent hole masses.[20] Their deduced equilibrium densities are shown in Fig. 11 along with our T=2K calculations. The density variations follow the linewidths of Fig. 10. At high stresses the experimental values are significantly smaller than theory. A similar but less pronounced difference was also found for Ge in Fig. 8. The importance of the discrepancy should not be underestimated, since the infinite-stress theory should be better than the zero-stress theory due to the simplifications in the band structure. The relevant band structure features are the number of bands, the masses, and their anisotropy. The number of bands is known, and because the occupied bands are ellipsoidal for infinite stress the anisotropy can be incorporated in the masses.

We have investigated the effect of a uniform change in both electron and hole masses on the EHL equilibrium density.[27] We suppose that the masses change in the kinetic energy and that the exchange-correlation energies are unchanged. For a mass decrease of 10%, we find that the equilibrium densities decrease rather uniformly for all stresses by nearly 25% in Model 1 and by $\approx$35% in Model 2. The Fermi energies and the luminescence linewidth have a smaller decrease, $\approx$8%. On the other hand, in extracting the density by fitting a luminescence

spectrum, a given spectrum would be assigned a density about 15% larger. The net effect of these changes in Fig. 11 would be to bring both theoretical curves and the data nearly into coincidence at high stresses. Thus a reduction of the electron and hole masses by ~10% at high compressive stress could remove some of the current discrepancies between theory and experiment.

Let us examine several possibilities for changes in one or both masses. First, our calculation of the hole masses[28] ignored the effects of the split-off valence band and fourth-order (k^4) terms which have been discussed by Hasegawa.[59] We find that including the split-off valence band results in only a small change in the density-of-states hole mass at the stresses attained in experiments: ≈1.7% for $-\sigma = 165$ kgf/mm^2 along <100> in Si and for $-\sigma = 20$ kgf/mm^2 along <111> in Ge. In addition, this mechanism increases rather than decreases the hole mass.[60] The fourth-order terms become less important at high stresses. Second, the reduction in the average band gaps with stress should be accompanied by a decrease in the carrier masses. These decreases may be simply estimated using the $\vec{k}\cdot\vec{p}$ result $m^{-1} \sim E_g^{-1}$ and a typical value 10meV/kbar = 1meV mm^2/kgf for the change in E_g with stress. The relevant gaps are *direct* gaps, i.e., E_o~0.9eV and E_1~2.3eV in Ge[61] and E_o~4.2eV and E_2~4.5eV in Si.[62] At the highest stresses attained in experiments, the masses would decrease by ~1–2% in Ge and ~4% in Si. A third possibility is the renormalization of the carrier masses within the EHL by many-body effects. It has been found both theoretically[63,64] and experimentally[65,66] that for unstressed Ge the masses within the EHL increase by ≈10% relative to the bulk masses. The stress dependence of this mass renormalization is not known. We conclude that decreases in the carrier masses by as much as 10% at high stresses cannot be reliably predicted by these considerations.

The electron and hole Fermi energies for Si are shown in Fig, 12, where the solid circles indicate E_F^e and the open circles E_F^h. We find the following theoretical values for the critical stresses:

$$\left.\begin{aligned} -\sigma_e &\approx 10 \text{ kgf/mm}^2 \\ -\sigma_h &\approx 37 \text{ kgf/mm}^2 \end{aligned}\right\} \text{ Si, T=2K, <100> stress .} \qquad (14)$$

The qualitative theoretical behavior of E_F^e and E_F^h can be understood for Si in the same way as for Ge. We note that the dashed line which indicates E_{spl}^e crosses the experimental points near their maximum. A similar feature occurs in Fig. 9 for Ge. This deviation from theory may be associated with the inappropriate use of the equilibrium limit in this stress range. In spite of the *quantitative* differences between theory and experiment, we note that $E_F^h > E_F^e$ at all stresses. Thus EHD should be negatively charged at all stresses in Si, in contrast to the situation for Ge. There are no experimental results concerning the charge on EHD in Si.

Two experimental measurements of the EHL binding energy are available for stressed Si. Kulakovskii et al.[67] found $\phi = 2 \pm 0.2$ meV at a stress $-\sigma = 48$ kgf/mm^2. We find theoretical upper limits of 2.40 meV for Model 1 and 2.50 meV for Model 2. In addition, Wolfe and Gourley[68] measured $\phi = 1.5 \pm 0.5$ meV at a stress $-\sigma = 90$ kgf/mm^2, compared to 1.84 meV for Model 1 and 2.01 meV for Model 2. The agreement between theory and experiment is satisfactory: as expected, ϕ decreases at higher stresses.

We consider finally the the infinite-stress limit of the EHL in Ge and Si. This limit is important because the simplifications in the band structure should make theories more tractable. Since infinite stress is impossible to attain experimentally, it is necessary to understand what constitutes a stress "high enough" that the valence band nonparabolicity is negligible or to have a method for extrapolating to infinite stress. Our calculations show that the properties of the EHL are still changing at stresses much greater than σ_h. The T=2K equilibrium densities for Ge and Si are replotted as a function of $1/\sigma$ in Figs. 13 and 14, respectively, where the arrows indicate σ_h. Data points from the sources for Figs. 8[14,16–19] and 11[20] are also shown. In Ge, at $-\sigma = 20$ kgf/mm^2, the largest experimental stress to date, the theoretical densities are still twice their infinite-stress values. To obtain densities within 20% of the infinite-stress value, stresses in the range $-\sigma \gtrsim 70$ kgf/mm^2 would be required for Ge and $-\sigma \gtrsim 150$ kgf/mm^2 for Si.

Data for somewhat lower stresses can be used, however, to extrapolate to infinite stress. For example, Fig. 13 shows that a linear extrapolation (on an n vs. $1/\sigma$ semilog plot) would be appropriate for stresses greater than $\approx$15 kgf/mm^2. A different extrapolation procedure used by Thomas and Pokrovskii[18] was inappropriate because it was based on only a few data points, all obtained at rather low stresses. While the data of Zarate and Timusk[19] agree well with Model 2, their densities are larger than those obtained by Chou et al.[16,17] and should be treated with caution. Therefore, is not possible to make a reliable extrapolation to infinite stress based on current data for Ge. For Si, it is evident from Fig. 14 that such a linear extrapolation procedure should be reasonable for stresses above $\approx$40 kgf/mm^2. The data of Gourley and Wolfe[20] extend well into this range. Our extrapolation yields an infinite-stress density $n \approx 2.8\times10^{17}\text{cm}^{-3}$ ($T \approx 1.4$K in the experiments).

IV. Results: Finite Temperature

In this section we are interested in the variation of EHL properties with temperature. First we shall consider the systematic variations at low temperatures, which involve derivatives of ground-state properties. Then we will consider the critical point of the electron-hole liquid-gas system. Finally, we comment briefly on scaling relations for EHL parameters.

A. Low-Temperature Variations; Compressibility

The usual procedure for studying the properties of the EHL at low temperatures is a perturbation treatment. At sufficiently low temperatures, EHL properties vary as T^2, just like any other degenerate Fermi system. The systematic low-temperature variations depend on derivatives of ground-state properties. In this section we consider four quantities: the isothermal compressibility, K_T, and quantities which describe the low-temperature variations of the equilibrium density (δ_n), chemical potential (δ_μ), and total Fermi energy (δ_E).

The following definition of the isothermal compressibility is valid for any density and temperature:

$$K_T^{-1} \equiv -V \left(\frac{\partial P}{\partial V}\right)_{N,T}$$

$$= 2n^2 f'(n,T) + n^3 f''(n,T), \tag{15}$$

where the prime denotes differentiation with respect to density at constant temperature. The second line uses Eqs. (1b) and (9). For the ground state

$$K_T(n_o) = \left[n_o^3 f_G''\right]^{-1}, \tag{16}$$

where

$$f_G'' = f''(n_o,0) \tag{17}$$

is the curvature of the free energy. The ground state compressibilities for Models 1 and 2 are shown as a function of stress for Ge and Si in Figs. 15 and 16, respectively. The second derivative f_G'' was calculated numerically. The overall increase in $K_T(n_o)$ with stress is primarily due to the decrease in n_o. At densities just above those where the upper conduction and valence bands empty, the free energy is relatively flat so its curvature is relatively small, resulting in anomalous peaks in the compressibility. The anomalies occur just below the critical stresses σ_e and σ_h, and their size depends on how drastic the carrier redistribution is. Because the predicted increase in $K_T(n_o)$ just below σ_e is so large for both Ge and Si, experimental measurements in this range of stresses would be particularly interesting. Two measurements of the compressibility have been obtained in stressed Ge. We have found,[69] for T=1.9K and $-\sigma \approx 5.5$ kgf/mm^2, that $K_T \approx 0.067 \pm 0.017$ cm^2/dyne ($n \approx 0.47 \times 10^{17}$cm^{-3}), compared to a theoretical value of 0.041 cm^2/dyne for Model 1. In addition, Ohyama et al.[70] obtained $K_T \approx 0.023 \pm 0.002$ cm^2/dyne for $T = 0$ and a similar but unspecified stress. Because the latter authors did not take into account the compression of the liquid by the strain well, however, we believe that their result could underestimate the true value by as much as a factor of 3.[69] In view of the complexity of the measurements, the agreement is fairly good.

The parameters δ_n, δ_μ, and δ_E are defined from the following relations:[1]

$$n(T) = n_o \left[1 - \delta_n (kT)^2\right], \quad \delta_n \text{ in meV}^{-2} \tag{18a}$$

$$\mu(T) = \mu(0) - \delta_\mu (kT)^2, \quad \delta_\mu \text{ in meV}^{-1} \tag{18b}$$

$$E_F(T) = E_F(0) \left[1 - \delta_E (kT)^2\right], \quad \delta_E \text{ in meV}^{-2}. \tag{18c}$$

Because of the complications due to the band splitting and nonparabolicity, the derivation of these quantities will be outlined here. We use a T=O expression for the exchange-correlation energy, so the pair free energy for finite T can be written

$$f(n,T) = f_{kin}(n,T) + f_{excor}(n,0). \tag{19}$$

At low temperatures the kinetic energy can be rewritten as

$$f_{kin}(n,T) = f_{kin}(n,0) - \frac{1}{2}\gamma(n)T^2, \tag{20a}$$

where

$$\gamma(n) \equiv \frac{\pi^2}{3} k^2 \frac{D(E_F(0))}{N}. \tag{20b}$$

Note that γ is a function of density via the Fermi energy and that Eq. (20) can be used separately for electrons and holes. The density of states is given by Eq. (7). The quantity γ, which is related to the heat capacity, is a monotonically decreasing function of the density except in a narrow range of densities where the occupation of the upper ν_2 bands is small (but nonzero). At the density corresponding to $E_F(0) = E_{spl}$ the derivative $\gamma'(n)$ is discontinuous. Thus anomalies occur in quantities which depend on γ at stresses just below σ_e and σ_h.

We note that the validity of the low-temperature expansion requires $O < \frac{kT}{E_F(T)} \ll 1$ and $O < \frac{kT}{E_F(T) - E_{spl}} \ll 1$. For the special case $E_F = E_{spl}$, then, Eq. (20) is invalid. For other cases, these conditions may be fulfilled by restricting the expansion to sufficiently low

temperatures.

Equations (19) and (20a) may be combined to give

$$f(n,T) = f(n,0) - \frac{1}{2}\left[\gamma_e(n) + \gamma_h(n)\right]T^2, \tag{21}$$

writing out explicitly the electron and hole contributions to the low-temperature correction. If the equilibrium density at the temperature T is written

$$n(T) = n_o + \Delta n, \tag{22}$$

then the following equation is easily obtained:

$$f'(n_o + \Delta n, T) = 0 = \Delta n\, f''(n_o,0) - \frac{1}{2}\left[\gamma_e'(n_o) + \gamma_h'(n_o)\right]T^2, \tag{23}$$

to first order in Δn. Using Eqs. (16), (17), (18a), (22), and (23), δ_n may be written

$$\delta_n = -\frac{n_o^2 K_T(n_o)}{2k^2}\left[\gamma_e'(n_o) + \gamma_h'(n_o)\right]. \tag{24}$$

The results for δ_n are shown in Fig. 17a for Ge and in Fig. 18a for Si. The complicated stress dependence is of course a combination of the components in the formula. For most stresses γ_e and γ_h decrease as a function of density, so that δ_n is positive. Thus, as is familiar from unstressed Ge and Si, the electron-hole liquid expands with temperature. However, at stresses just below σ_e and σ_h, δ_n becomes negative, implying initial thermal contraction. Because of the restricted range of conditions for the thermal contraction and because of the difficulties associated with the measurement of all the δ quantities, the observation of a negative δ_n would be very difficult indeed (but very interesting).

The quantity δ_μ describes the variation in the chemical potential with temperature. At a low-temperature equilibrium density the chemical potential can be written

$$\mu(T) \equiv \mu(n(T),T) = f(n_o+\Delta n,T)$$

$$= \mu(0) - \frac{1}{2}\left[\gamma_e(n_o) + \gamma_h(n_o)\right]T^2, \tag{25}$$

to first order in Δn. Here we have used Eqs. (1c), (21), (22), and the fact that f is a minimum at a low-temperature equilibrium density. Using the definition in Eq. (18b),

$$\delta_\mu = \frac{1}{2k^2}\left[\gamma_e(n_o) + \gamma_h(n_o)\right]. \tag{26}$$

The results for Ge and Si are shown in Figs. 17b and 18b, respectively. The enhancement just below σ_e and σ_h shows the behavior of $\gamma_e(n)$ and $\gamma_h(n)$, respectively, at the associated densities. The broader σ_e-related structures in Si, as compared to Ge, reflect the more gradual emptying of the upper electron valleys. The discontinuity at σ_e for Model 1 in Ge arises from the discontinuity in the density.

The quantity δ_E describes the variation in the total Fermi energy $E_F^{tot} = E_F^e + E_F^h$ with temperature. There are actually two distinct contributions to the change in a (hole or electron) Fermi energy: the first is due to the change in equilibrium density with temperature, while the second is an explicit temperature dependence at constant density.[1] Thus we may write[27]

$$E_F(T) = E_F(0) + \Delta E_1 + \Delta E_2, \tag{27}$$

where

$$\Delta E_1 = -\, n_o\, \delta_n\, E_F'(0)\, (kT)^2 \tag{28a}$$

and

$$\Delta E_2 = -\frac{\pi^2}{6}\frac{D'(E_F(0))}{D(E_F(0))}(kT)^2 . \tag{28b}$$

In Eq. (28a) the prime indicates a derivative with respect to density, while in Eq. (28b) the prime indicates a derivative with respect to energy. These expressions are true for electrons or

for holes, with separate (additive) contributions required. The parameter δ_E may be written as follows, using Eqs. (18c), (27), and (28):

$$\delta_E = \delta_{E1} + \delta_{E2}, \tag{29a}$$

where

$$\delta_{E1} = \delta_n \, n_o \frac{E_F^{e'}(0) + E_F^{h'}(0)}{E_F^e(0) + E_F^h(0)} \tag{29b}$$

and

$$\delta_{E2} = \frac{\pi^2}{6} \frac{\dfrac{D'(E_F^e(0))}{D(E_F^e(0))} + \dfrac{D'(E_F^h(0))}{D(E_F^h(0))}}{E_F^e(0) + E_F^h(0)}. \tag{29c}$$

For most stresses δ_E is dominated by the first contribution, which is due to the change in the equilibrium density. Just below σ_e and σ_h, however, the second contribution becomes more important, because of the rapid change in the density of states at the Fermi level. The results for δ_E are shown in Fig. 17c for Ge and in Fig. 18c for Si. These curves are very similar to the curves for δ_n in Figs. 17a and 18a, with the exception just mentioned. Note that it is easy to verify that the expressions for δ_n, δ_μ, and δ_E in Eqs. (24), (26), and (29) simplify for unstressed Ge and Si to the usual expressions.[1]

Numerical results for $K_T(n_o)$ and the δ quantities are listed in Table IV for the same models and stresses as in Table III. In comparing Models 1 and 2, it is useful to remember that the quantities in the table depend on derivatives of the free energy (or a related quantity) and sometimes on high powers of the equilibrium density. Close agreement requires very detailed similarities between the models.

Measurements of the quantities discussed in this section are sparse. Zero-stress values are listed in the table and are in reasonable agreement with theory. Feldman et al.[15] found $\delta_n = 6.7 \pm 2.0$ meV^{-2} at 13 kgf/mm^2 in Ge, to be compared to theoretical values of 5.1 and

3.4 meV^{-2} for Models 1 and 2, respectively. Kulakovskii et al.[71] found $\delta_n = 0.21 \pm 0.3$ meV^{-2} for Si at an unspecified stress, probably in the range 50-80 kgf/mm^2. The corresponding theoretical values are $\approx$0.18 and $\approx$0.24 meV^{-2} for Models 1 and 2, respectively. No experimental values for δ_μ or δ_E have been published for either stressed Ge or stressed Si.

B. The Critical Point

Thermodynamically, the definition of the critical point is

$$\left(\frac{\partial P}{\partial V}\right)_{T,N} = \left(\frac{\partial^2 P}{\partial V^2}\right)_{T,N} = 0, \tag{30a}$$

which may be rewritten using Eqs. (1b), (1c), and (9):

$$\left(\frac{\partial \mu}{\partial n}\right)_T = \left(\frac{\partial^2 \mu}{\partial n^2}\right)_T = 0. \tag{30b}$$

Thus the critical point corresponds to the inflection point in the chemical potential versus density. By performing the calculation for a plasma of electrons and holes, we assume that other species such as excitons, trions, and biexcitons are not important near the critical point. This scheme was first used by Combescot[8] and has been followed in other calculations of the critical point at zero and infinite stress.

The finite-temperature kinetic energy contribution was computed exactly, as described in Section IIA, and temperature-independent exchange-correlation energies were used. In addition, in order to obtain meaningful results for Model 1, it was necessary to modify the correlation energies. As shown in Figs. 1 and 2 the Model 1 correlation energies contain slight anomalies which result from the polynomial fit; these anomalies are greatly magnified in the second and third derivatives which determine the critical point. To circumvent this mathematical problem we fitted the original Model 1 correlation energies to a simple Wigner form, consisting of a single term in Eq. (12), over an intermediate density range corresponding

to r_s=2 to 3, and then extended the calculation to higher and lower densities as needed. This procedure is reasonable since the correlation energy is expected to have a Wigner-type density dependence for $r_s>2$.[32] The modified Model 1 exchange-correlation energies are shown as dashed curves in Figs. 1 and 2.

The results for the critical temperature T_c and critical density n_c in Ge are shown in Figs. 19 and 20, respectively, while the results for Si are shown in Figs. 21 and 22. The results for Models 1 and 2 are quite similar, considering the sensitivity of the calculation to details such as curvature of the correlation energy. The qualitative stress dependences are analogous to the behavior of ground-state properties: gradual decreases in both T_c and n_c with stress, with a more rapid change associated with the depopulation of the upper electron valleys and a leveling off at high stresses where the valence-band changes become more gradual. The reduction in T_c with stress follows from the reduction in the liquid binding energy ϕ, while the decrease in n_c approximately parallels the decrease in the ground state density n_o except in the immediate vicinity of σ_c.

Numerical results for the critical point at selected values of the stress are given in Table IV, where they are compared to other calculations of the critical point. We show in the table the results of a T^2 calculation for Model 5 at zero stress and Model 6 at infinite stress. These models are practically identical to those used by Vashishta, Das, and Singwi[7] but the results differ substantially. This is due to an error in the calculation of Ref. 7 and those results have now been revised, in agreement with the values in the table.[29,32] We show for comparison the results of Reinecke et al.[72] calculated using their noninteracting fluctuation model,[73] which also uses a T^2 expansion. The values for T_c obtained in this model are lower than those obtained using the plasma model, while the values for n_c are consistently larger. Within the plasma model, the T^2 expansion overestimates both T_c and n_c, compared to the corresponding exact-T calculation. Other theoretical estimates[8,9,74,75] of the critical point in unstressed or infinitely stressed Ge and Si using different approximations for the exchange-correlation energy are in remarkably good agreement with the values in the table. Also, Liu and Liu[23] have calculated

the critical point at two values of the stress for Ge and Si, using energy-dependent masses and a T^2 expansion for the kinetic energy. Taking this into account, their results are in reasonable agreement with our calculations for the same stresses.

We wish to reiterate the systematic differences mentioned above between T^2 and exact-T calculations. The low-T expansion is only valid if $O < \frac{kT}{E_F} \ll 1$ and $O < \frac{kT}{E_F - E_{spl}} \ll 1$ for both electrons and holes. We find that these conditions are violated at the critical point for all stresses in both Ge and Si: the ratios fall outside the ranges (0 to 0.25) and (0 to 0.75) for Models 1 and 2, respectively, in Ge and outside the range (0 to 1) for both models in Si. In view of this, we find it surprising that the differences between the two types of estimates are not larger.

Experimental measurements of the critical point in unstressed Ge and Si are listed in Table IV. Measurements for stressed Ge include those of Furneaux et al.[49] ($T_c = 4.7-5.7$K for $-\sigma \approx 6$ kgf/mm^2) and Feldman et al.[15] ($T_c = 3.5 \pm 0.5$K and $n_c = 7.7 \pm 2.0 \times 10^{15}$cm^{-3} for $-\sigma = 13$ kgf/mm^2). These measurements are in reasonable agreement with the present calculations. In <100>-stressed Si, Forchel et al.[76] found $T_c = 14.0 \pm 0.5$K and $n_c = 1.8 \pm 0.3 \times 10^{17}$cm^{-3} for $-\sigma = 35$ kgf/mm^2. Kulakovskii et al.[71] found $T_c = 14 \pm 1.5$K for an unspecified stress, probably in the range $-\sigma = 50-80$ kgf/mm^2. Finally, Gourley and Wolfe[20,68] find $T_c = 12-22$K for $-\sigma = 90$ kgf/mm^2 and $T_c \gtrsim 20$K for $-\sigma = 163$ kgf/mm^2. Until the large experimental discrepancies are resolved it is difficult to make meaningful comparisons with theory.

C. Scaling Relations

We comment briefly on scaling relations of properties of electron-hole liquids. An early suggestion was made[1] that certain combinations of EHL properties should scale from one system (i.e., band structure) to another. More recently, Reinecke and Ying[77] have proposed on the basis of theoretical arguments a revised set of scaling quantities. They assume that the

conduction and valence bands are parabolic and that the exchange-correlation energy can be written $f_{excor} \sim n^p$, using the same value of p for different systems. In this model the proposed scaling quantities are n_c/n_o, $|f_G|/\kappa T_c$, and $\kappa T_c/n_o^p\,(\kappa/\mu)^{1-3p}$, where μ is an optical average of the electron and hole masses, in units of the free electron mass. In addition, they propose that $p \approx 0.25$.

The validity of these ideas can easily be tested by computing the above quantities as a function of stress for Ge and Si, using Models 1 and 2. We find the following ranges of values:

$$\frac{n_c}{n_o} \approx 0.08 - 0.14 \tag{31a}$$

$$\frac{|f_G|}{kT_c} \approx 7.8 - 10.2 \tag{31b}$$

$$\frac{T_c\kappa}{n_o^{1/4}}\left(\frac{\kappa}{\mu}\right)^{1/4} \approx 0.016 - 0.025 \text{ K cm}^{3/4}\,. \tag{31c}$$

We have excluded from consideration a small range of stresses around σ_e, where we find somewhat larger variations. The ratio n_c/n_o, in particular, changes rapidly in the vicinity of σ_e, as can be seen by comparing Figs. 3 and 4 with Figs. 20 and 22. The values obtained for these quantities using the fluctuation model[77] are different from the present values obtained using the plasma model for the critical point. The experimental values given in Tables III and IV for unstressed Ge, for which there is good agreement among different experiments, seem to favor the fluctuation model. However, the variations with stress, exchange-correlation energy model, and material from Eq. (31) are expected to persist. We find, for example, that the extreme values for the scaling quantities are not necessarily obtained at zero or infinite stress. We conclude that the "universal" scaling quantities, originally proposed for model systems, have somewhat more variation when considered as functions of stress. This undoubtedly occurs because the simple form for the free energy used in Ref. 77 is not applicable at finite stresses.

Acknowledgements

I am grateful for assistance and advice from R. S. Markiewicz during the early phases of this work, and for many discussions with P. Vashishta concerning his unpublished calculations. I would also like to thank P. L. Gourley and H. G. Zarate for sending their experimental results prior to publication. D. E. Aspnes, J. C. Hensel, and T. M. Rice provided helpful comments on the manuscript. The work performed at Berkeley was supported in part by the Director, Office of Energy Research, Office of Basic Energy Sciences, Material Sciences Division of the U. S. Department of Energy under Contract Number W-7405-ENG-48.

References

1. For reviews, see the articles by T. M. Rice and by J. C. Hensel, T. G. Phillips and G. A. Thomas in *Solid State Physics*, edited by H. Ehrenreich, F. Seitz and D. Turnbull, Vol. 32 (Academic Press, 1977), pp. 1 and 88.

2. M. Combescot and P. Nozières, J. Phys. C *5*, 2369 (1972).

3. W. F. Brinkman and T. M. Rice, Phys. Rev. B*7*, 1508 (1973).

4. P. Bhattacharyya, V. Massida, K. S. Singwi and P. Vashishta, Phys. Rev. B*10*, 5127 (1974).

5. P. Vashishta, P. Bhattacharyya and K. S. Singwi, Phys. Rev. B*10*, 5108 (1974).

6. P. Vashishta, R. K. Kalia and K. S. Singwi, *Lecture Notes in Physics*, edited by M. Ueta and Y. Nishina, Vol. 57 (Springer-Verlag, Heidelberg, 1976), p. 187.

7. P. Vashishta, S. G. Das and K. S. Singwi, Phys. Rev. Lett. *33*, 911 (1974).

8. M. Combescot, Phys. Rev. Lett. *32*, 15 (1974).

9. G. A. Thomas, T. M. Rice, and J. C. Hensel, Phys. Rev. Lett. *33*, 219 (1974).

10. V. S. Bagaev, T. I. Galkina, O. V. Gogolin and L. V. Keldysh, Pisma Zh. Eksp. Teor. Fiz. *10*, 309 (1969) [JETP Lett. *10*, 195 (1969)]; V. S. Bagaev, T. I. Galkina and O. V. Gogolin, *Proc. X Int'l. Conf. on Phys. Semic., Cambridge*, edited by S. P. Keller, J. C. Hensel and F. Stern (USAEC, 1970), p. 500.

11. C. Benôit à la Guillaume, M. Voos and F. Salvan, Phys. Rev. B*5*, 3079 (1972).

12. B. M. Ashkinadze, I. P. Kretsu, A. A. Patrin and I. D. Yaroshetskii, Fiz. Tekh. Poluprovodn. *4*, 2206 (1970) [Soviet Phys. - Semic. *4*, 1897 (1970)].

13. R. S. Markiewicz, J. P. Wolfe and C. D. Jeffries, Phys. Rev. Lett. *32*, 1357 (1974); *34*, 59(E) (1975); J. P. Wolfe, R. S. Markiewicz, C. Kittel and C. D. Jeffries, Phys. Rev. Lett. *34*, 275 (1975); C. D. Jeffries, J. P. Wolfe, S. M. Kelso, R. S. Markiewicz and J. E.

Furneaux, J. Lumin. *12*, 659 (1976).

14. J. P. Wolfe, R. S. Markiewicz, S. M. Kelso, J. E. Furneaux and C. D. Jeffries, Phys. Rev. B*18*, 1479 (1978).

15. B. J. Feldman, H.-h. Chou and G. K. Wong, Solid State Commun. *24*, 521 (1977).

16. B. J. Feldman, H.-h. Chou and G. K. Wong, Solid State Commun. *26*, 209 (1978).

17. H.-h. Chou and G. K. Wong, Phys. Rev. Lett. *41*, 1677 (1978).

18. G. A. Thomas and Ya. E. Pokrovskii, Phys. Rev. B*18*, 864 (1978).

19. H. G. Zarate, Thesis, McMaster University (1981) (unpublished); H. G. Zarate and T. Timusk, Bull. Amer. Phys. Soc. *26*, 487 (1981) and to be published.

20. P. L. Gourley, Thesis, University of Illinois at Urbana-Champaign (1980) (unpublished); P. L. Gourley and J. P. Wolfe, to be published.

21. R. S. Markiewicz and S. M. Kelso, Solid State Commun. *25*, 275 (1978).

22. L. Liu, Solid State Commun. *25*, 805 (1978).

23. L. Liu and L. S. Liu, Solid State Commun. *27*, 801 (1978).

24. G. Kirczenow and K. S. Singwi, Phys. Rev. B*19*, 2117 (1979).

25. G. Kirczenow and K. S. Singwi, Phys. Rev. B*21*, 3597 (1980).

26. Some of the results are indicated in S. M. Kelso, Bull. Amer. Phys. Soc. *24*, 343 (1979).

27. S. M. Kelso, Thesis, University of California, Berkeley (1979) (unpublished).

28. S. M. Kelso, Phys. Rev. B (in press).

29. P. Vashishta, R. K. Kalia and K. S. Singwi, in *Electron-Hole Droplets in Semiconductors*, edited by L. V. Keldysh and C. D. Jeffries (North-Holland, to be published); P. Vashishta and R. K. Kalia, to be published.

30. G. Kirczenow and K. S. Singwi, Phys. Rev. Lett. *41*, 326 (1978); 1140 (E) (1978).

31. M. Combescot, Phys. Rev. B*10*, 5045 (1974).

32. P. Vashishta, private communication (1977).

33. R. K. Kalia and P. Vashishta, Phys. Rev. B*17*, 2655 (1978).

34. P. Vashishta, private communication (1978).

35. The form of the correlation energy is very similar to that given in Ref. 33 except that the power series contains more terms and is valid for a wider range of densities.

36. H. Büttner, *Festkörperprobleme XIII*, edited by H. J. Queisser (Pergamon, Vieweg, 1973), p. 145; E. P. Wigner, Trans. Faraday Soc. *34*, 678 (1938).

37. A controversy concerning the best values of the deformation potentials for Si apparently remains unresolved (J. C. Hensel, private communication).

38. W. Kohn and J. M. Luttinger, Phys. Rev. *97*, 1721 (1955); *98*, 915 (1955).

39. N. O. Lipari and M. Altarelli, Phys. Rev. B*15*, 4883 (1977).

40. V. I. Sidorov and Ya. E. Pokrovskii, Fiz. Tekh. Poluprovodn. *6*, 2405 (1972) [Soviet Phys. - Semic. *6*, 2015 (1973)].

41. K. L. Shaklee and R. E. Nahory, Phys. Rev. Lett. *24*, 942 (1970).

42. T. Ohyama, T. Sanada and E. Otsuka, Phys. Rev. Lett. *33*, 647 (1974).

43. B. M. Ashkinadze, I. P. Kretsu, A. A. Patrin and I. D. Yaroshetskii, Phys. Stat. Sol. (b) *46*, 495 (1971).

44. E. A. Andryushin, O. A. Gel'fond and A. P. Silin, Fiz. Tverd. Tela *22*, 1418 (1980) [Soviet Phys. - Solid State *22*, 827 (1980)].

45. A. A. Kastal'skii, Fiz. Tverd. Tela *20*, 1241 (1978) [Soviet Phys. - Solid State *20*, 715 (1978)].

46. F. Bassani and D. Brust, Phys. Rev. *131*, 1524 (1963).

47. P. Merle, D. Auvergne, H. Mathieu and J. Chevallier, Phys. Rev. B*15*, 2032 (1977).

48. K. Y. Cheng, G. L. Pearson, R. S. Bauer and D. J. Chadi, Bull. Amer. Phys. Soc. *21*, 365 (1976).

49. J. E. Furneaux, R. S. Markiewicz and S. M. Kelso, Bull. Amer. Phys. Soc. *22*, 270 (1977).

50. T. M. Rice, Phys. Rev. B9, 1540 (1974).

51. Ya. E. Pokrovskii and K. I. Svistunova, Zh. Eksp. Teor. Fiz. Pis. Red. *19*, 92 (1974) [JETP Lett. *19*, 56 (1974)]; Fiz. Tverd. Tela *16*, 3399 (1974) [Soviet Phys. - Solid State *16*, 2202 (1975)]; *Proc. XII Int'l. Conf. on Phys. Semic., Stuttgart*, edited by M. H. Pilkuhn (Teubner, Stuttgart, 1974), p. 71.

52. The luminescence spectra obtained by Ya. E. Pokrovskii and K. I. Svistunova, Zh. Eksp. Teor. Fiz. *68*, 2323 (1975) [Soviet Phys. - JETP *41*, 1161 (1976)] are analyzed in Ref. 18.

53. R. B. Hammond, T. C. McGill and J. W. Mayer, Phys. Rev. B*13*, 3566 (1976).

54. V. D. Kulakovskii, V. B. Timofeev and V. M. Edel'shtein, Zh. Eksp. Teor. Fiz. *74*, 372 (1978) [Soviet Phys. JETP *47*, 193 (1978)]; V. M. Edel'shtein, V. D. Kulakovskii and V. B. Timofeev, *Physics of Semiconductors 1978*, Inst. Phys. Conf. Ser. No. 43, edited by B. L. H. Wilson (Inst. Phys., London, 1979), p. 383.

55. J. Wagner and R. Sauer, Phys. Stat. Sol. (b) *94*, 69 (1979).

56. J. Wagner, A. Forchel and R. Sauer, Solid State Commun. *36*, 917 (1980).

57. A. Forchel, B. Laurich, G. Moersch, W. Schmid and T. L. Reinecke, Phys. Rev. Lett. *46*, 678 (1981).

58. The measurements of Ξ_u in the following papers differ by only ~10%: I. Balslev, Phys.

Rev. *143*, 636 (1966); L. Laude, F. H. Pollak and M. Cardona, Phys. Rev. B*3*, 2623 (1971); I. P. Akimchenko and V. A. Vdovenkov, Fiz. Tverd. Tela *11*, 658 (1969) [Soviet Phys. - Solid State *11*, 528 (1969)]; K. Murase, K. Enjouji and E. Otsuka, J. Phys. Soc. Jpn. *29*, 1248 (1970).

59. H. Hasegawa, Phys. Rev. *129*, 1029 (1963).

60. J. C. Hensel and G. Feher, Phys. Rev. *129*, 1041 (1963); J. C. Hensel and K. Suzuki, Phys. Rev. B*9*, 4219 (1974).

61. D. E. Aspnes, Phys. Rev. B*12*, 2297 (1975).

62. A. Daunois and D. E. Aspnes, Phys. Rev. B*18*, 1824 (1978).

63. T. M. Rice, Il Nuovo Cimento *23B*, 226 (1974).

64. M. Rösler and R. Zimmermann, Phys. Stat. Sol. (b) *67*, 525 (1975).

65. H. L. Störmer, R. W. Martin and J. C. Hensel, *Proc. XIII Int'l. Conf. on Phys. Semic., Rome*, edited by F. G. Fumi (Tipografia Marves, Rome, 1976), p. 950; R. W. Martin, H. L. Störmer, W. Ruhle and D. Bimberg, J. Lumin. *12/13*, 645 (1976); H. L. Störmer and R. W. Martin, *Proc of the Conf. on the Application of High Mag. Fields in Semic. Physics, Oxford*, edited by J. F. Ryan (Clarendon Laboratory, Oxford, UK, 1978), p. 269.

66. V. I. Gavrilenko, V. L. Kononenko, T. S. Mandel'shtam and V. N. Murzin, Pis'ma Zh. Eksp. Teor. Fiz. *23*, 701 (1976) [JETP Lett. *23*, 645 (1976)].

67. See Ref. 54. The value for ϕ should be fairly accurate in spite of the incorrect procedure used to analyze the EHL lineshape, since one is concerned only with the location of the high-energy edge of the spectrum.

68. J. P. Wolfe and P. L. Gourley, *Physics of Semiconductors 1978*, Inst. Phys. Conf. Ser. No. 43, edited by B. L. H. Wilson (Inst. Phys., London, 1979), p. 379.

69. S. M. Kelso, to be published.

70. T. Ohyama, I. Honbori and E. Otsuka, J. Phys. Soc. Jpn. *48*, 1559 (1980).

71. V. D. Kulakovskii, I. V. Kukushkin and V. B. Timofeev, Zh. Eksp. Teor. Fiz. *78*, 381 (1980) [Soviet Phys. - JETP *51*, 191 (1980)].

72. T. L. Reinecke, M. C. Lega and S. C. Ying, Phys. Rev. B*20*, 1562 (1979).

73. T. L. Reinecke and S. C. Ying, Phys. Rev. B*13*, 1850 (1976).

74. W. D. Kraeft and W. Fennel, Phys. Stat. Sol. (b) *73*, 487 (1976).

75. T. L. Reinecke, M. C. Lega and S. C. Ying, Phys. Rev. B*20*, 5404 (1979).

76. A. Forchel, B. Laurich, G. Moersch, W. Schmid and T. L. Reinecke, Phys. Rev. Lett. *46*, 678 (1981).

77. T. L. Reinecke and S. C. Ying, Phys. Rev. Lett. *43*, 1054 (1979).

Table I. Parameters used in the calculations.

Parameter	Ge	Ref	Si	Ref
Electrons				
m_{et}/m_o	0.08152	a	0.1905	b
m_{el}/m_o	1.588	a	0.9163	b
m_{de}/m_o	0.2193	c	0.3216	c
m_{oe}/m_o	0.1192	d	0.2588	d
$\phi(\rho_e)$	0.8401	e	0.9490	e
ν_e(zero stress)	4		6	
ν_e(infinite stress)	1 (<111> stress)		2 (<100> stress)	
$-E^e_{spl}/\sigma$	1.05	f	0.86	f
Holes				
$\psi(\rho_h)$(zero stress)	0.710	g	0.746	g
$-E^h_{spl}/\sigma$	0.362	h	0.272	h
Holes: infinite stress	<111> stress		<100> stress	
m_{ht}/m_o	0.1302	i	0.2561	i
m_{hl}/m_o	0.04037	i	0.1989	i
m_{dh}/m_o	0.08811	c	0.2354	c
m_{oh}/m_o	0.07474	d	0.2337	d
$\psi(\rho_h)$	0.9698	e	0.9986	e
Miscellaneous				
κ	15.36	j	11.40	j
a(Model 2)	0.1917	k	0.2128	k
c(Model 2)	4.461	k	8.552	k

Table I Refs.

a. B. W. Levinger and D. R. Frankl, J. Phys. Chem. Solids *20*, 281 (1961).

b. J. C. Hensel, H. Hasegawa, and M. Nakayama, Phys. Rev. *138*, A225 (1965).

c. $m_d = (m_t^2 m_\ell)^{1/3}$ for electrons or holes.

d. $m_o^{-1} = \frac{1}{3}(2m_t^{-1} + m_\ell^{-1})$ for electrons or holes.

e. M. Combescot and P. Nozières, J. Phys. C *5*, 2369 (1972).

f. Units: meV mm^2/kgf. For <111> stress (Ge), $-E^e_{spl}/\sigma = 4\frac{\Xi_u}{9C_{44}}$. For <100> stress (Si), $-E^{\prime}_{spl}\sigma = \frac{\Xi_u}{C_{11}-C_{12}}$. Values for Ξ_u are from I. Balslev, Phys. Rev. *143*, 636 (1966). Values for the C's for Ge are from M. E. Fine, J. Appl. Phys. *26*, 862 (1965) (T=1.7K). Values for the C's for Si are from H. J. McSkimin, J. Appl. Phys. *24*, 988 (1953) (T=78K values multiplied by 1.002 to extrapolate to low temperature).

g. W. F. Brinkman and T. M. Rice, Phys. Rev. B*7*, 1508 (1973).

h. Units: meV mm^2/kgf. For <111> stress (Ge), $-E^h_{spl}/\sigma = \frac{d}{\sqrt{3}C_{44}}$. For <100> stress (Si), $-E^h_{spl}/\sigma = \frac{2b}{C_{11}-C_{12}}$. Values for d (Ge) and b (Si) are from J. C. Hensel and K. Suzuki, Phys. Rev. B*9*, 4219 (1974) and from J. C. Hensel and G. Feher, Phys. Rev. *129*, 1041 (1963), respectively. Values for the C's are as in Ref. f.

i. Calculated from Ge and Si valence band structures: see S. M. Kelso, Phys. Rev. B (in press), Rev. 28.

j. R. A. Faulkner, Phys. Rev. *184*, 713 (1969).

k. Model 2 is described in the text. If n has units $10^{17}cm^{-3}$ and the masses are multiples of the free electron mass, then a is dimensionless and c is in meV.

Table II. Electron and hole treatments in the exchange-correlation energy models.

Model	Type	Exchange Energy		Correlation Energy	
		Electrons	Holes	Electrons	Holes
1	FSC	infinite stress	zero stress	infinite stress	zero stress
2	Wigner	infinite stress	zero stress	infinite stress	infinite-stress optical mass
3	Wigner	infinite stress	zero stress	infinite stress	stress-dependent optical mass
4	Wigner	infinite stress	zero stress	infinite stress	stress-dependent density-of-states mass
5	FSC	zero stress	zero stress	zero stress	zero stress
6	FSC	infinite stress	infinite stress	infinite stress	infinite stress

Table III. Selected numerical results for the ground state properties of the EHL in stressed Ge and Si.

Material, Stress Direction	$-\sigma$ (kgf/mm^2)	Model	n_o (10^{17} cm^{-3})	$-f_G$ (meV)	E_F^e (meV)	E_F^h (meV)	$K_T(n_o)$ (cm^2/dyne)
Ge, <111>	Zero	Expt.[a]	2.3±0.1	6.1±0.2	2.53±0.02	3.90±0.02	$(2.3\pm0.6)\times10^{-3}$
		5	2.21	5.88	2.40	3.73	3.12×10^{-3}
		1	2.70	6.14	2.75	4.27	2.31×10^{-3}
		2	2.24	6.03	2.43	3.77	2.87×10^{-3}
	3	1	0.642	4.06	2.66	2.16	1.80×10^{-2}
		2	0.659	4.06	2.71	2.19	1.38×10^{-2}
	7	1	0.435	3.66	2.05	2.32	3.75×10^{-2}
		2	0.492	3.65	2.23	2.45	2.42×10^{-2}
	20	1	0.200	3.22	1.22	2.19	9.05×10^{-2}
		2	0.259	3.15	1.45	2.49	5.98×10^{-2}
	Infinite	1	0.098	2.96	0.76	1.92	1.25×10^{-1}
		2	0.112	2.82	0.83	2.10	1.09×10^{-1}
		6	0.109	3.07	0.81	2.06	1.39×10^{-1}
Si, <100>	Zero	Expt.[a]	33±1	23	7.8±0.1	14.4±0.1	$(3.4\pm2)\times10^{-5}$
		5	32.3	21.97	7.50	13.79	5.96×10^{-5}
		1	31.8	22.52	7.43	13.64	6.69×10^{-5}
		2	29.3	22.42	7.03	12.91	6.47×10^{-5}
	12	1	13.6	17.42	8.75	9.32	1.58×10^{-4}
		2	13.1	17.42	8.55	9.14	1.78×10^{-4}
	40	1	9.04	15.47	6.68	10.25	2.88×10^{-4}
		2	8.18	15.54	6.25	9.74	3.98×10^{-4}
	100	1	6.22	14.60	5.20	9.94	4.22×10^{-4}
		2	5.41	14.78	4.74	9.17	5.63×10^{-4}
	Infinite	1	4.74	14.09	4.34	9.46	5.50×10^{-4}
		2	4.20	14.35	4.01	8.73	6.40×10^{-4}
		6	4.46	14.71	4.17	9.08	5.99×10^{-4}

a The experimental data at zero stress are compiled from J. C. Hensel, T. G. Phillips, and G. A. Thomas, *Solid State Physics*, ed. by H. Ehrenreich, F. Seitz, and D. Turnbull, Vol. 32 (Academic Press, 1977), p. 88.

Table IV. Selected numerical results for properties of the EHL in stressed Ge and Si at finite temperature.

Material, Stress Direction	$-\sigma$ (kgf/mm^2)	Model	δ_n (meV^{-2})	δ_μ (meV^{-1})	δ_E (meV^{-2})	T_c (K)	n_c (10^{17} cm^{-3})
Ge, <111>	Zero	Expt.	0.9-1.4[a,b]	2.2±0.9[b]	0.71±0.14[b]	6.5-7.0[f,g,h]	0.5-1.0[f,g,h]
		5	1.24	1.69	0.92	8.18[j]	0.50[j]
		Fluc.				6.73[k]	0.66[k]
		1	0.98	1.47	0.73	6.95	0.28
		2	1.15	1.67	0.85	7.96	0.31
	3	1	2.91	2.41	1.91	5.05	0.065
		2	2.25	2.37	1.52	5.92	0.087
	7	1	3.90	2.75	2.47	4.59	0.042
		2	2.67	2.57	1.76	5.39	0.062
	20	1	5.65	3.53	3.61	3.95	0.018
		2	4.19	3.07	2.66	4.53	0.028
	Infinite	1	5.94	4.53	4.52	3.61	0.010
		2	5.41	4.14	4.07	3.99	0.014
		6	6.84	4.23	5.05	3.72[j]	0.017[j]
		Fluc.				2.91[k]	0.032[k]
Si, <100>	Zero	Expt.	0.055±0.020[c,d]	0.3-1.7[c,d,e]	0.05±0.025[c,d,e]	26-30[e,i],22-24[l]	10-14[e,i,l]
		5	0.104	0.508	0.078	28.6[j]	5.1[j]
		Fluc.				23.5[k]	9.6[k]
		1	0.117	0.513	0.086	27.4	3.7
		2	0.110	0.542	0.082	26.7	3.5
	12	1	0.136	0.599	0.094	23.2	1.7
		2	0.152	0.613	0.104	22.6	1.6
	40	1	0.169	0.685	0.113	20.4	0.90
		2	0.222	0.727	0.146	20.0	0.82
	100	1	0.193	0.750	0.135	19.2	0.63
		2	0.246	0.823	0.175	18.8	0.58
	Infinite	1	0.231	0.829	0.174	18.6	0.52
		2	0.258	0.898	0.196	18.3	0.48
		6	0.246	0.864	0.186	24.4[j]	0.78[j]
		Fluc.				14.2[k]	1.42[k]

a. T. K. Lo, Sol. St. Comm. *15*, 1231 (1974).

b. G. A. Thomas, T. G. Phillips, T. M. Rice, and J. C. Hensel, Phys. Rev. Lett. *31*, 386 (1973).

c. R. B. Hammond, T. C. McGill, and J. W. Mayer, Phys. Rev. B *13*, 3566 (1976).

d. M. A. Vouk and E. C. Lightowlers, J. Phys. C *8*, 3695 (1975).

e. A. F. Dite, V. D. Kulakovskii, and V. B. Timofeev, Zh. Eksp. Teor. Fiz. *72*, 1156 (1977) [Sov. Phys. -- JETP *72*, 604 (1977)].

f. G. A. Thomas, T. M. Rice, and J. C. Hensel, Phys. Rev. Lett. *33*, 219 (1974).

g. W. Miniscalco, C.-C. Huang, and M. B. Salamon, Phys. Rev. Lett. *39*, 1356 (1977).

h. G. A. Thomas, J. B. Mock, and M. Capizzi, Phys. Rev. B *18*, 4250 (1978).

i. J. Shah, M. Combescot, and A. H. Dayem, Phys. Rev. Lett. *38*, 1497 (1977).

j. Computed using T^2 expansion. The values differ from those given in P. Vashishta, S. G. Das, and K. S. Singwi, Phys. Rev. Lett. *33*, 911 (1974), as explained in the text.

k. Computed using droplet-fluctuation model. T. L. Reinecke, M. C. Lega, and S. C. Ying, Phys. Rev. B *20*, 1562 (1979).

l. A. Forchel, B. Laurich, G. Moersch, W. Schmid, and T. L. Reinecke, Phys. Rev. Lett. *46*, 678 (1981).

Figure Captions

Fig. 1. Exchange-correlation energy per electron-hole pair for Models 1, 5, and 6, normalized to Model 2, for <111>-stressed Ge. The dashed curve is discussed in Section IVB.

Fig. 2. As Figure 1, for <100>-stressed Si.

Fig. 3. Ground-state density n_0 versus stress σ for the EHL in <111>-stressed Ge. (a) Models 1, 5, and 6; (b) Models 2, 3, and 4. The arrows indicate the Model 5 zero-stress and Model 6 infinite-stress densities.

Fig. 4. As Figure 3, for <100>-stressed Si.

Fig. 5. Ground-state electron-hole pair energy versus stress for the EHL in <111>-stressed Ge. The dashed line is the infinite-stress exciton binding energy.

Fig. 6. As Figure 5, for <100>-stressed Si.

Fig. 7. Equilibrium density versus stress for Ge-like bands with one lower and ν_2 upper electron valleys. The Model 1 exchange-correlation energy is used.

Fig. 8. Equilibrium density versus stress for Ge at T=2K. The curves are the results for Models 1 and 2. The data points are taken from Refs. 18 (●), 16(▼), 17 (▲), 14 (+), and 19 (■).

Fig. 9. Electron and hole Fermi energies, E_F^e and E_F^h, versus stress for Ge at T=2K. The dot-dashed curves are Model 1, while the solid curves are Model 2. The dashed lines indicate the energy splitting, E_{spl}, between upper and lower bands for electrons and for holes. The data points for E_F^e (solid symbols) and E_F^h (open symbols) are from Refs. 18 (circles) and 17 (triangles).

Fig. 10. Luminescence linewidth versus stress for the EHL in <100>-stressed Si at T=2K. The curves are the results for Models 1 and 2. The data points are taken from Refs. 53 (◆), 54 (■), 55 (▲), 56 (▼), 57 (▶), and 20 (●).

Fig. 11. Equilibrium density versus stress for Si at T=2K. The curves are the results for Models 1 and 2, and the data points are from Ref. 20.

Fig. 12. Electron and hole Fermi energies versus stress for Si at T=2K. Notation for the curves is similar to Fig. 9, while the data points for E_F^e (•) and E_F^h (o) are from Ref. 20.

Fig. 13. Equilibrium density versus $1/\sigma$ for Ge at T=2K. The curves are the results for Models 1 and 2, and the data points are the same as in Fig. 8. The arrow indicates the critical stress σ_h.

Fig. 14. As Figure 13, for Si. The data points are from Ref. 20.

Fig. 15. Isothermal compressibility of the EHL ground state as a function of <111> stress in Ge, for Models 1 and 2.

Fig. 16. As Figure 15, for <100> stress in Si.

Fig. 17. (a) δ_n, (b) δ_μ, (c) δ_E as a function of <111> stress for Ge. Models 1 and 2 are shown.

Fig. 18. As Figure 17, for <100> stress in Si.

Fig. 19. EHL critical temperature versus <111> stress in Ge, according to Models 1 and 2.

Fig. 20. EHL critical density versus <111> stress in Ge, for Models 1 and 2.

Fig. 21. EHL critical temperature versus <100> stress in Si, for Models 1 and 2.

Fig. 22. EHL critical density versus <100> stress in Si, according to Models 1 and 2.

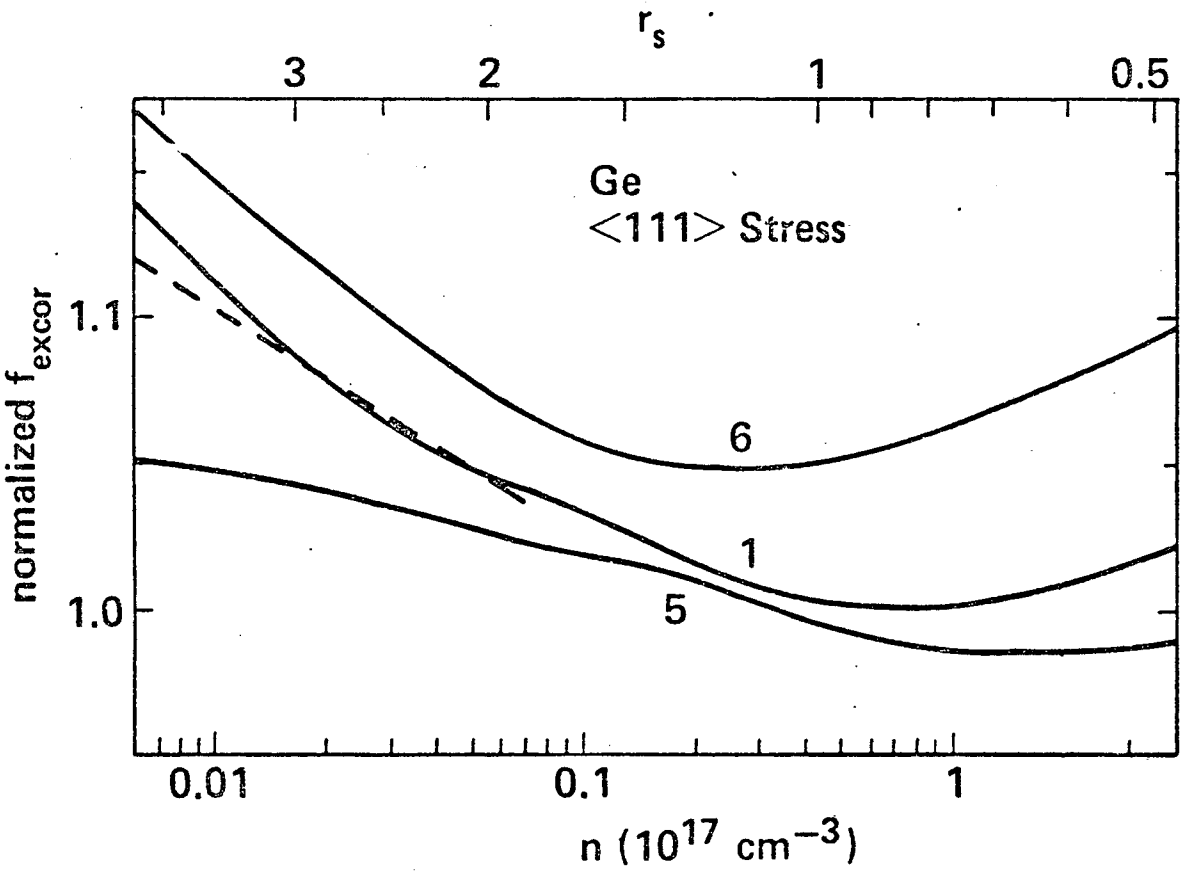
r_s
3
2
1
0.5
Ge
<111> Stress
normalized f_{excor}
1.1
1.0
6
1
5
0.01
0.1
1
n (10^{17} cm^{-3})

FIG. 1

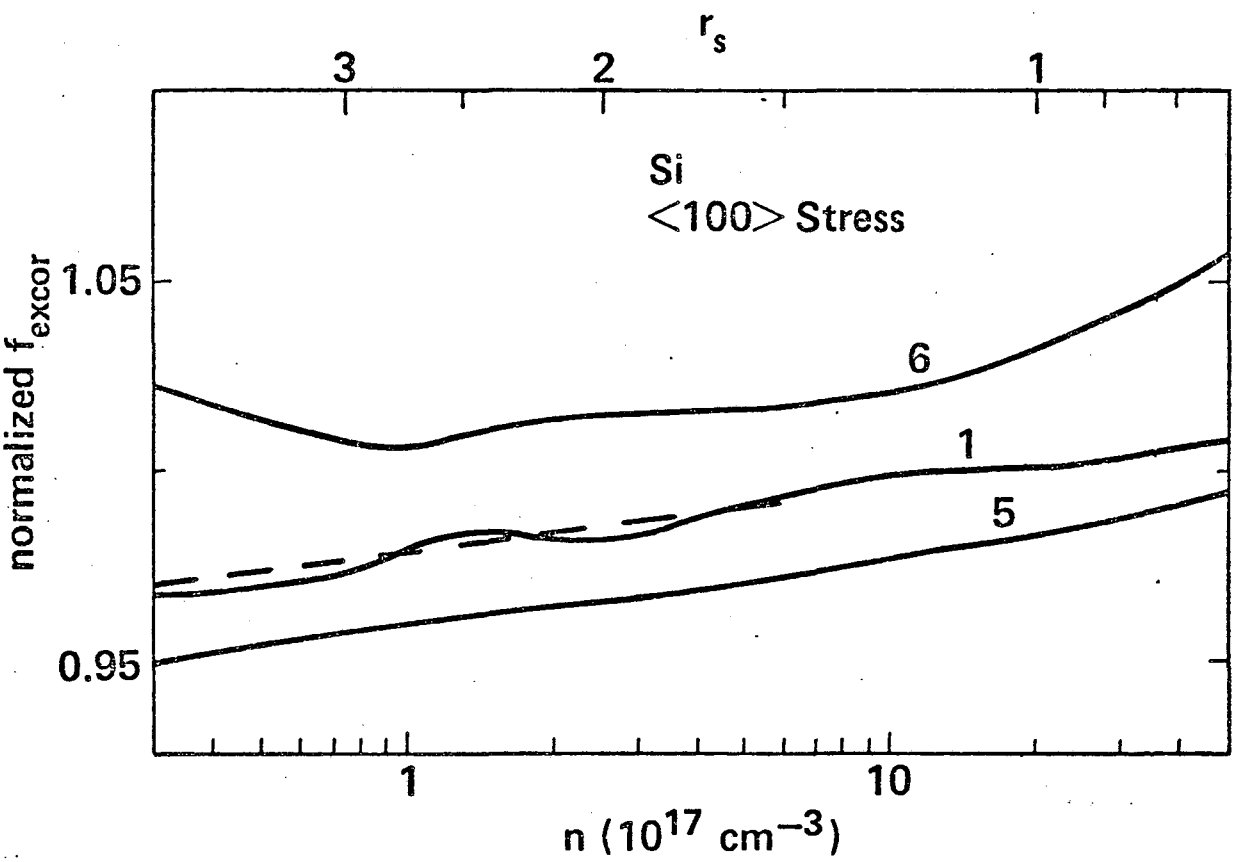
r_s
3
2
1
Si
<100> Stress
normalized f_{excor}
1.05
0.95
6
1
5
1
10
n (10^{17} cm^{-3})

FIG. 2

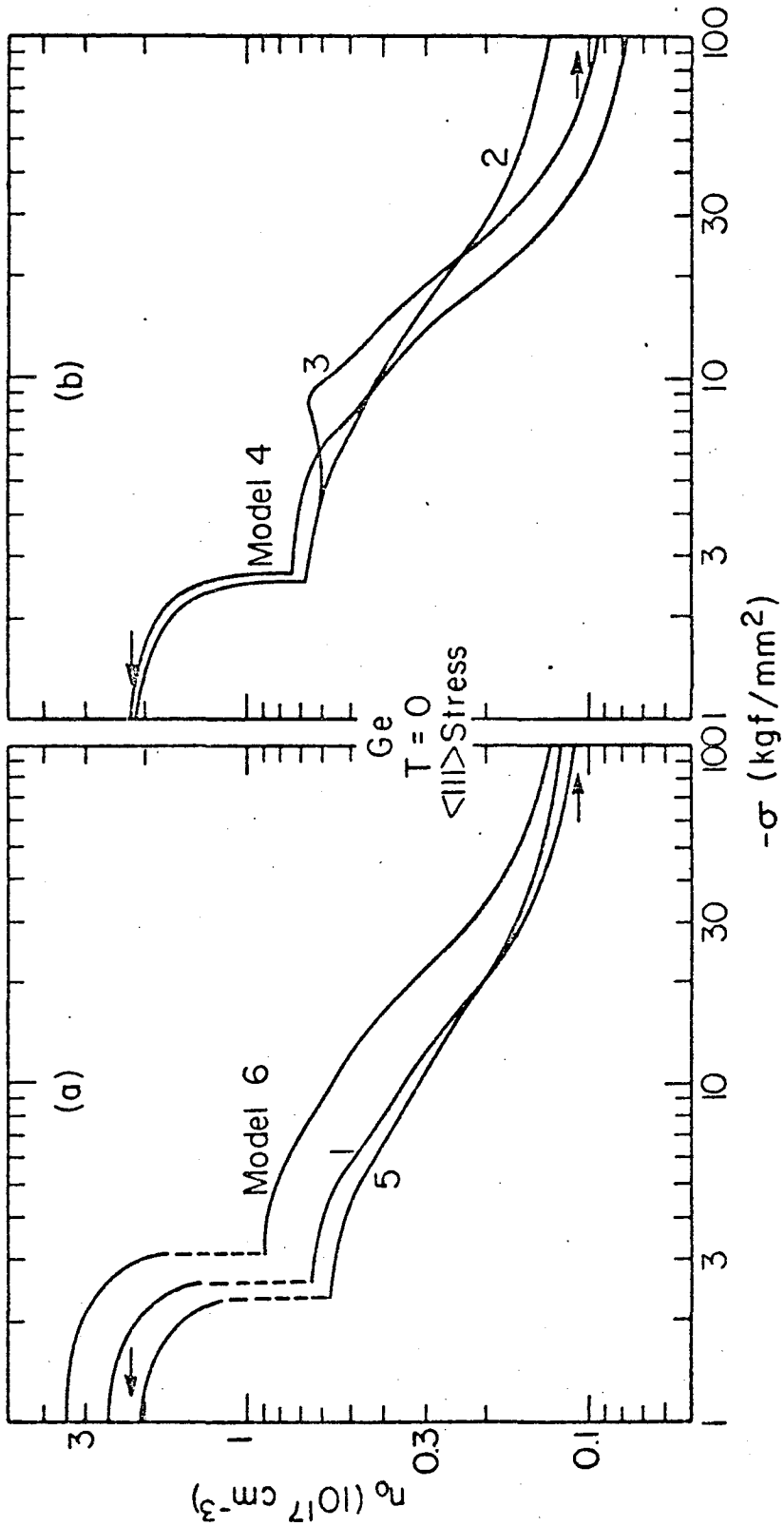
(a)
Model 6
1
5
(b)
Model 4
2
3
Ge
T = 0
<111>Stress
n_0 (10^{17} cm^{-3})
3
1
0.3
0.1
1
3
10
30
100
$-\sigma$ (kgf/mm^2)

FIG. 3

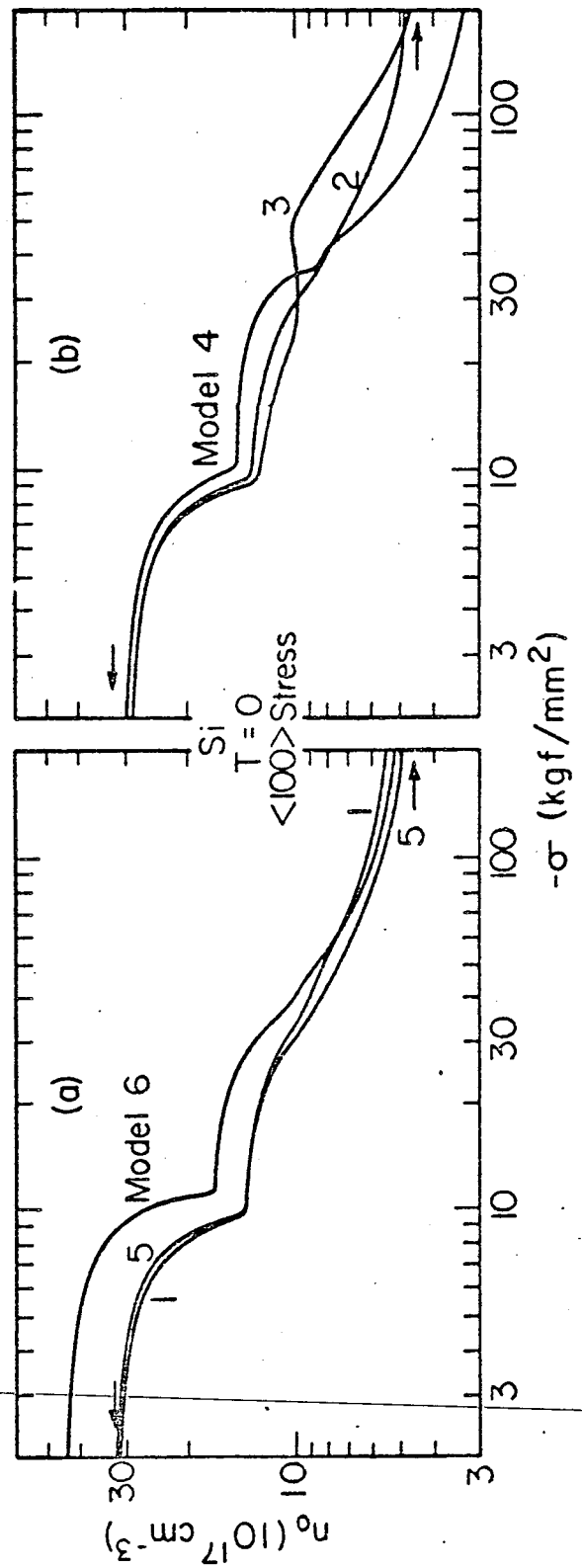
(a)
Model 6
5
1
5
1
(b)
Model 4
3
2
Si
T = 0
<100> Stress
n_o (10^{17} cm^{-3})
$-\sigma$ (kgf/mm^2)
3
10
30
100

FIG. 4

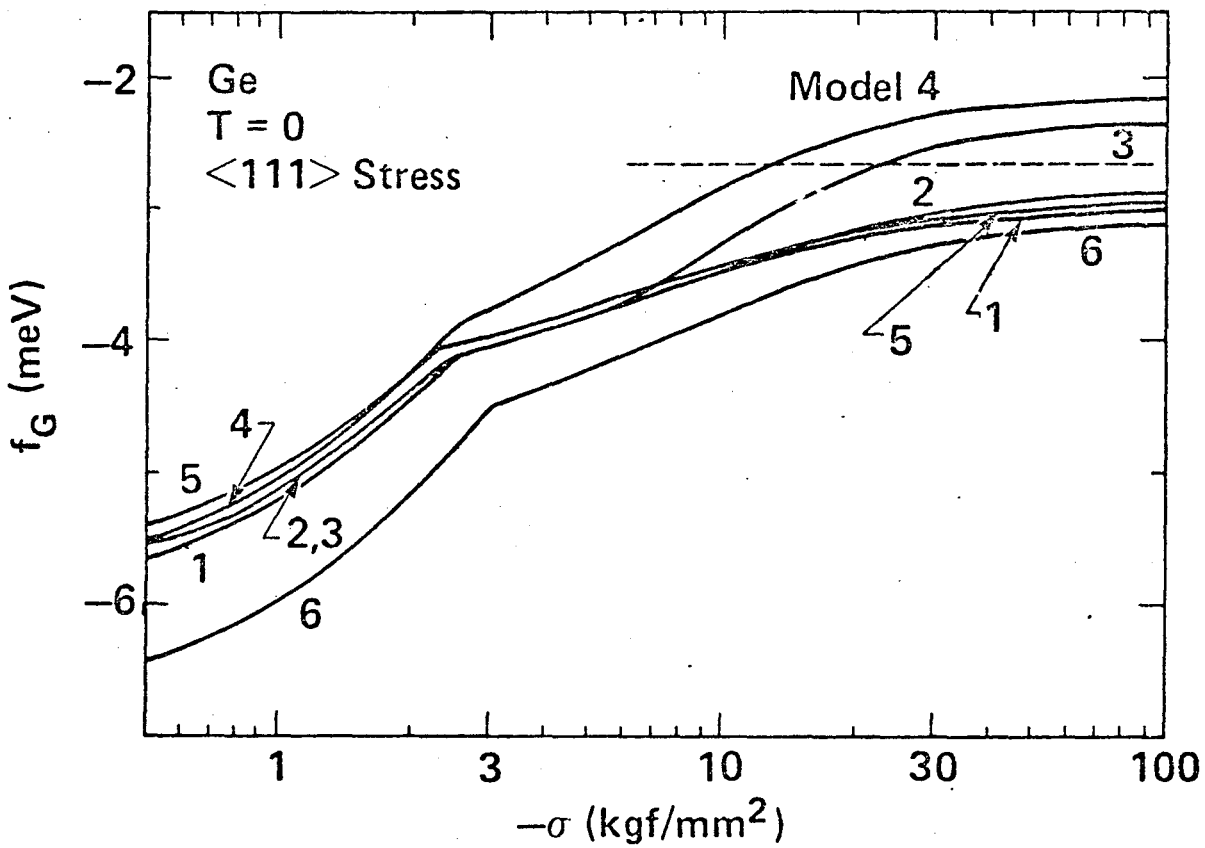
Ge
T = 0
<111> Stress
Model 4
3
2
6
5
1
4
5
2,3
1
6
−2
−4
−6
f_G (meV)
1
3
10
30
100
$-\sigma$ (kgf/mm^2)

FIG. 5

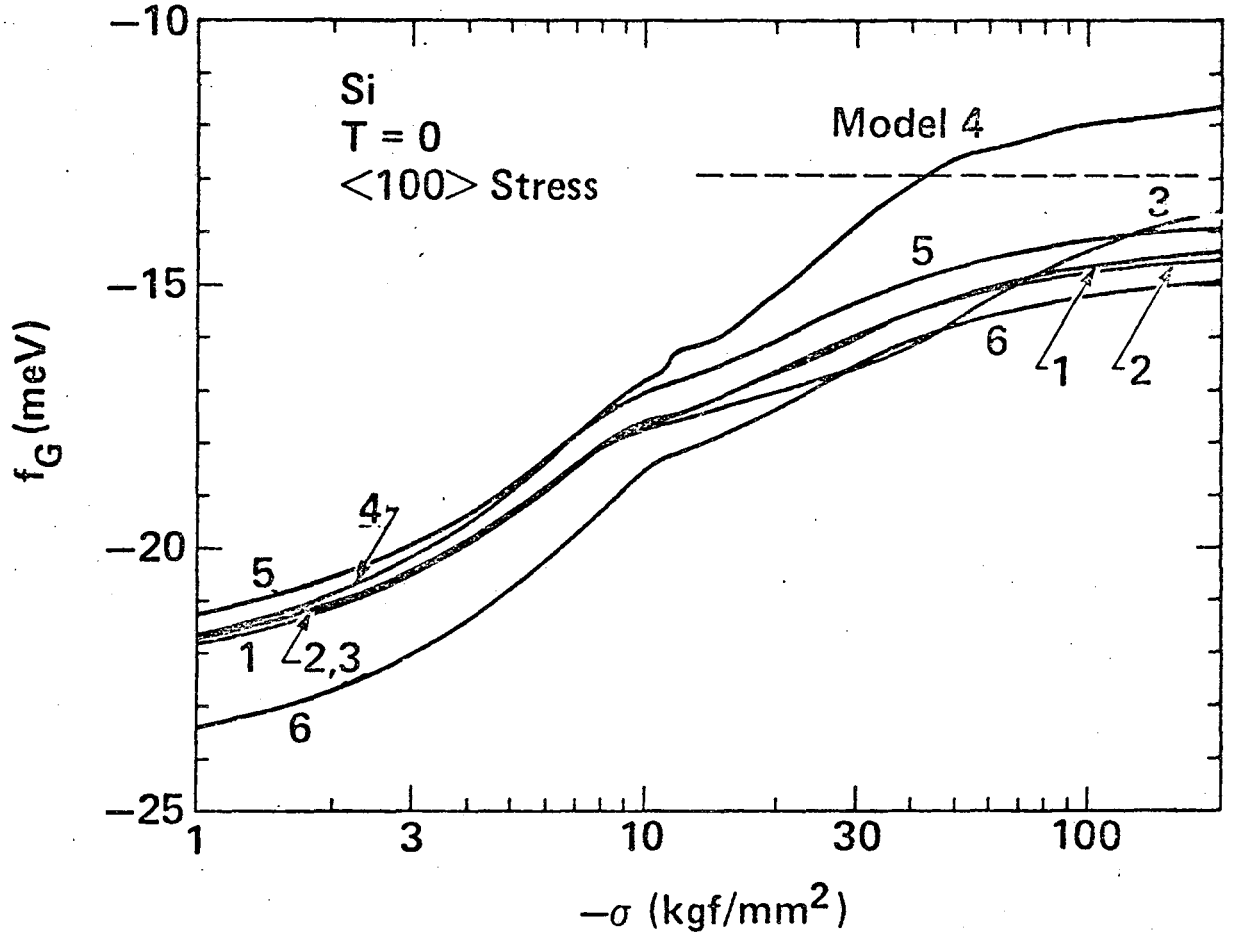
Si
T = 0
<100> Stress
Model 4
−10
−15
−20
−25
1
3
10
30
100
f_G (meV)
$-\sigma$ (kgf/mm^2)
1
2,3
4
5
6
5
6
1
2
3

FIG. 6

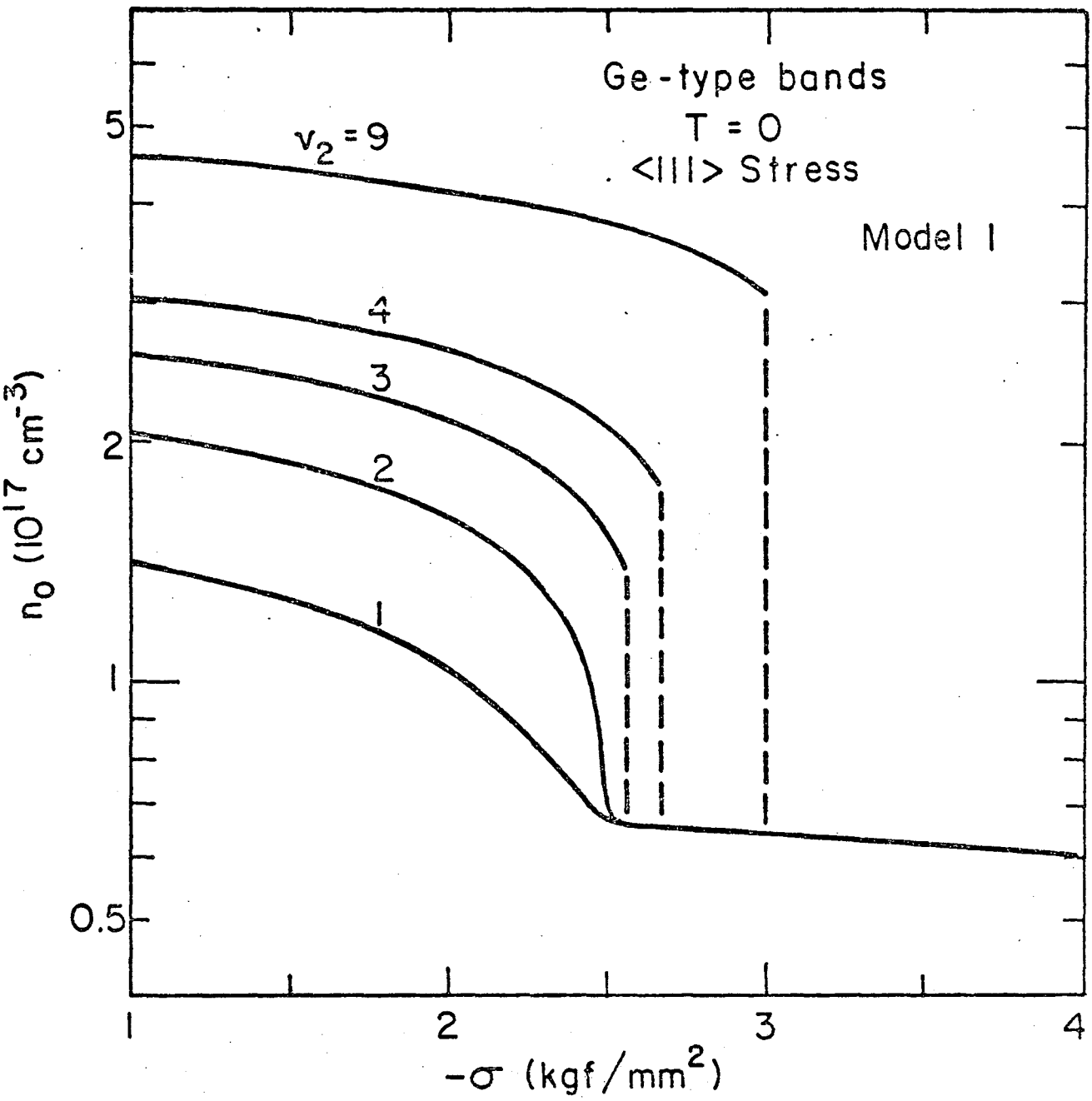
Ge-type bands
T = 0
<111> Stress
Model I
$\nu_2 = 9$
4
3
2
1
5
2
1
0.5
n_0 (10^{17} cm^{-3})
1
2
3
4
$-\sigma$ (kgf/mm^2)

FIG. 7

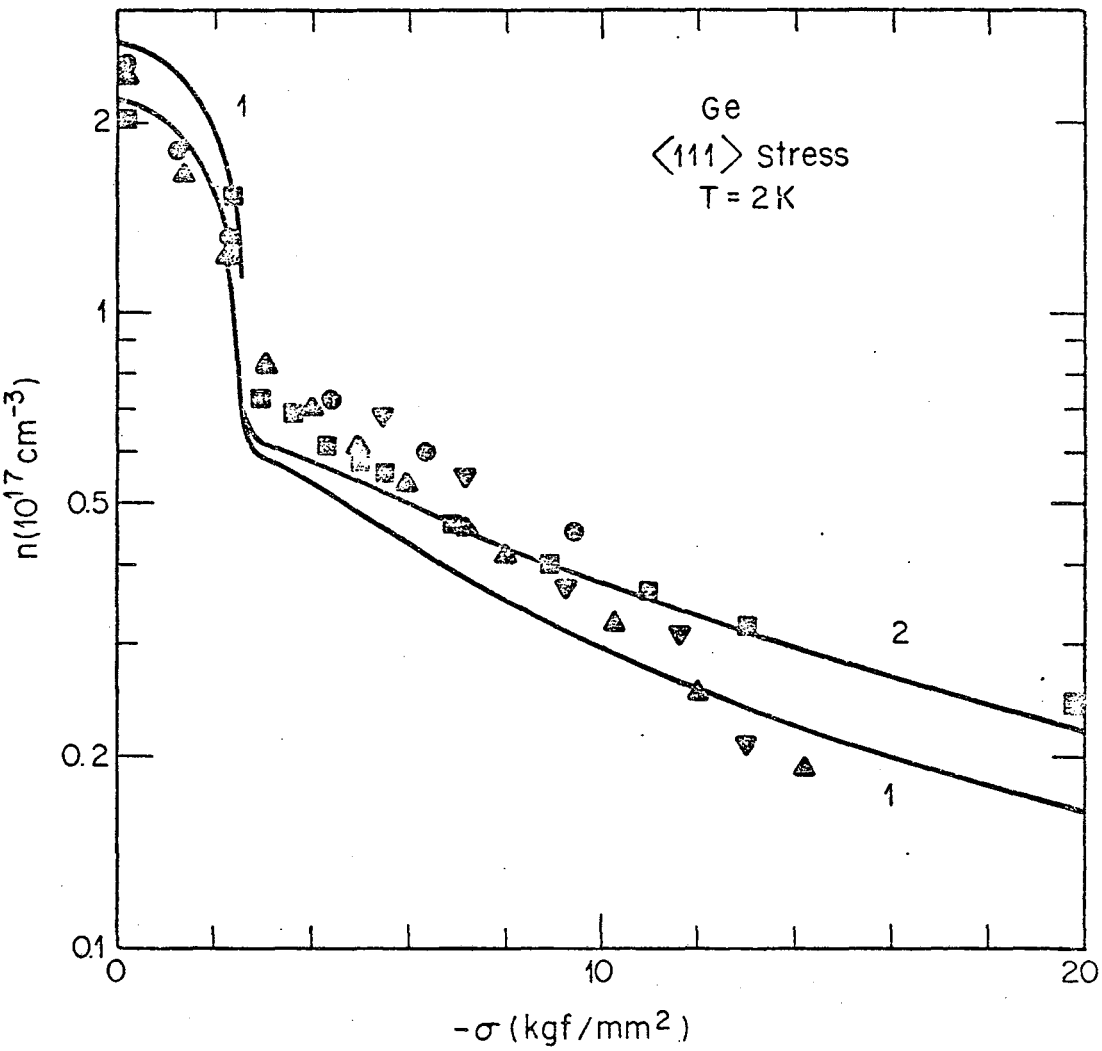

FIG. 8

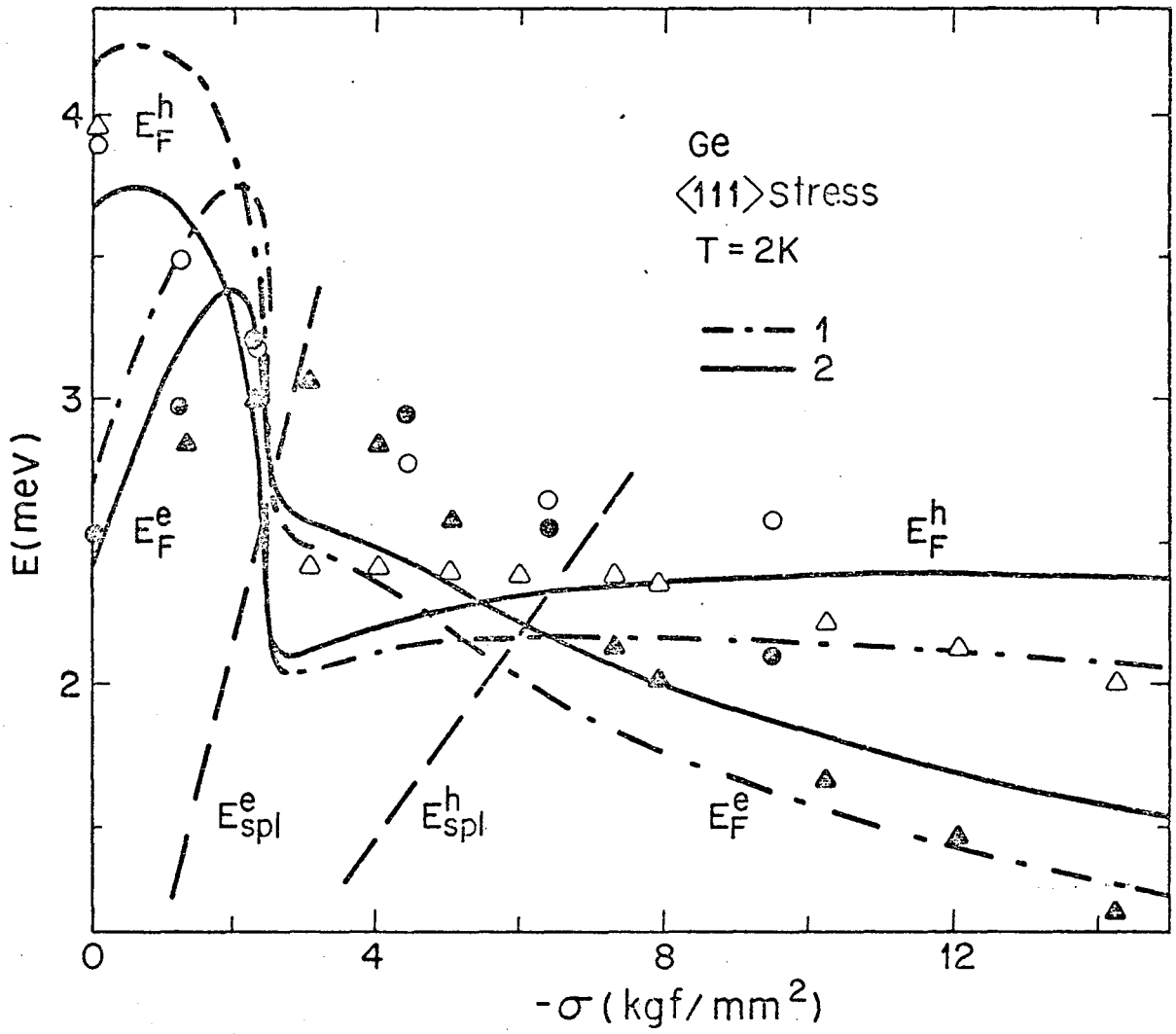
Ge
⟨111⟩ Stress
T = 2K
1
2
E_F^h
E_F^e
E_{spl}^e
E_{spl}^h
E_F^h
E_F^e
E(meV)
4
3
2
0
4
8
12
$-\sigma$ (kgf/mm^2)

FIG. 9

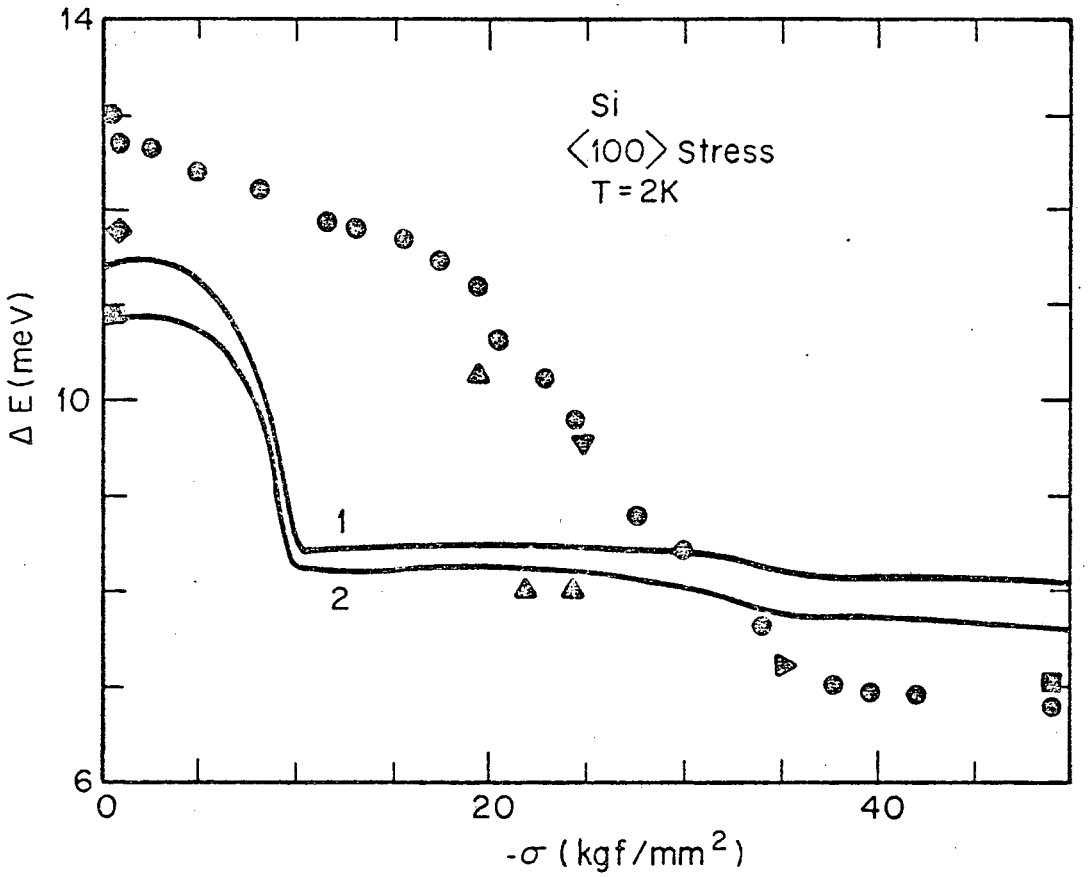

FIG. 10

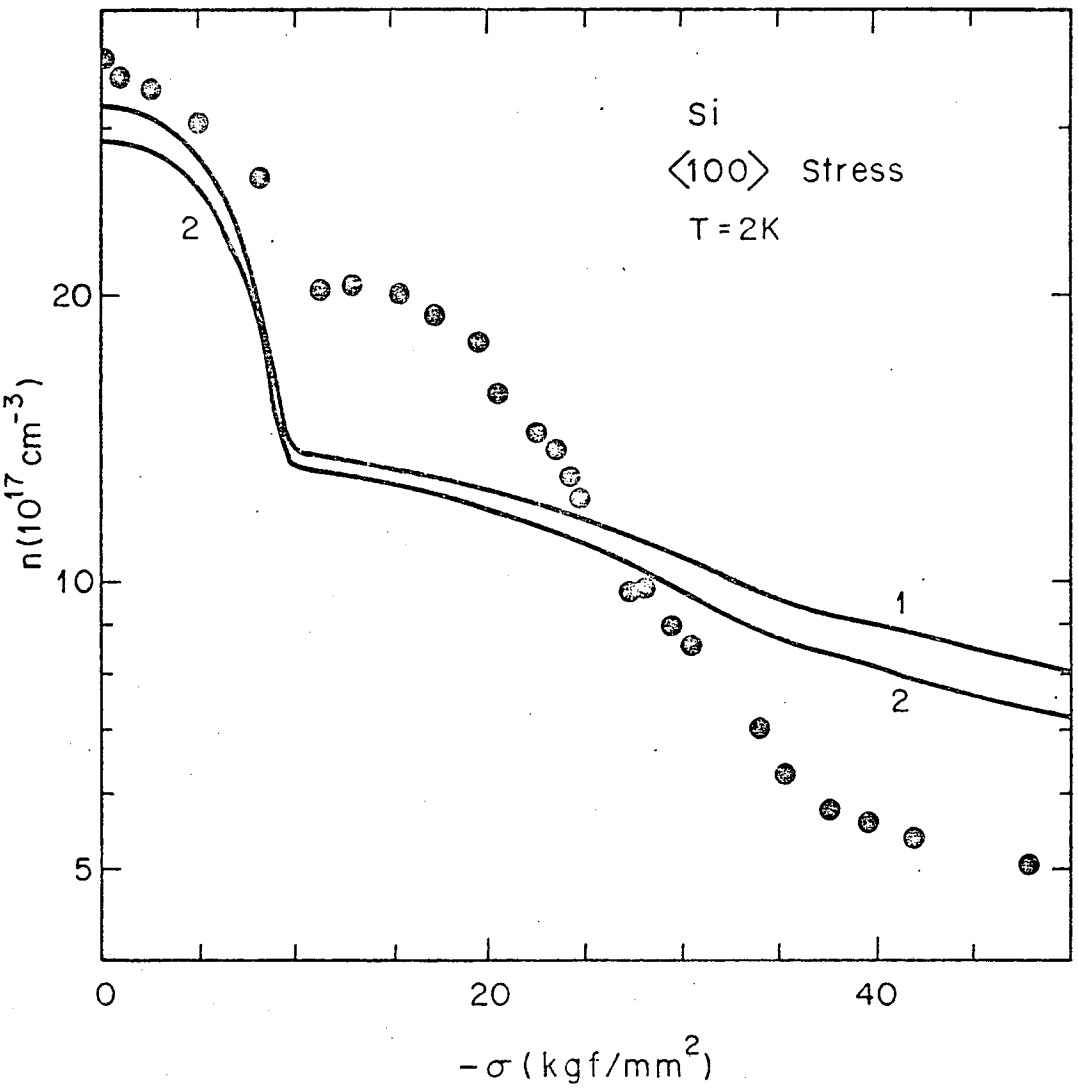

FIG. 11

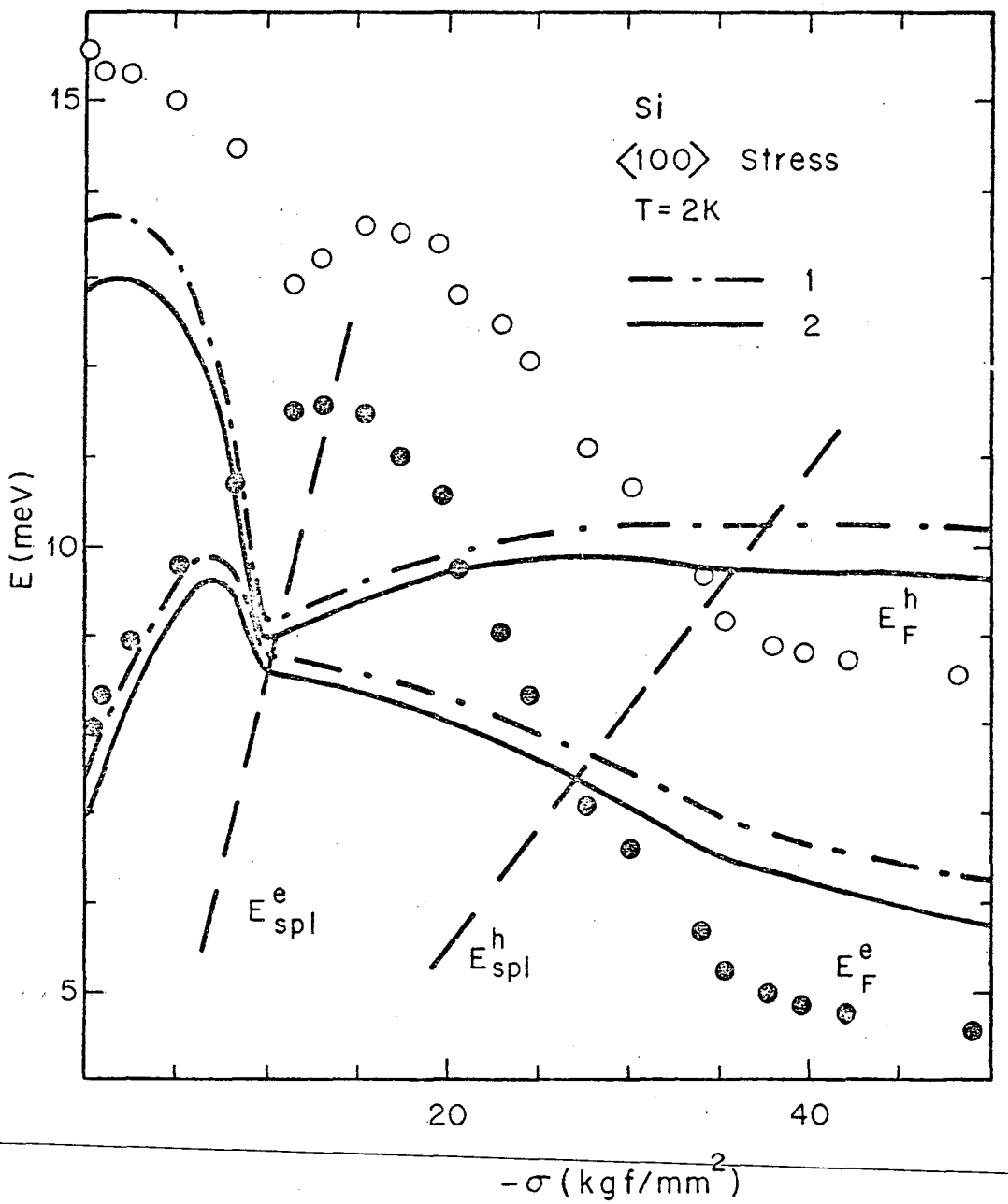
Si
⟨100⟩ Stress
T = 2K
1
2
15
10
5
E (meV)
20
40
$-\sigma$ (kgf/mm^2)
E^h_F
E^e_F
E^e_{spl}
E^h_{spl}

FIG. 12

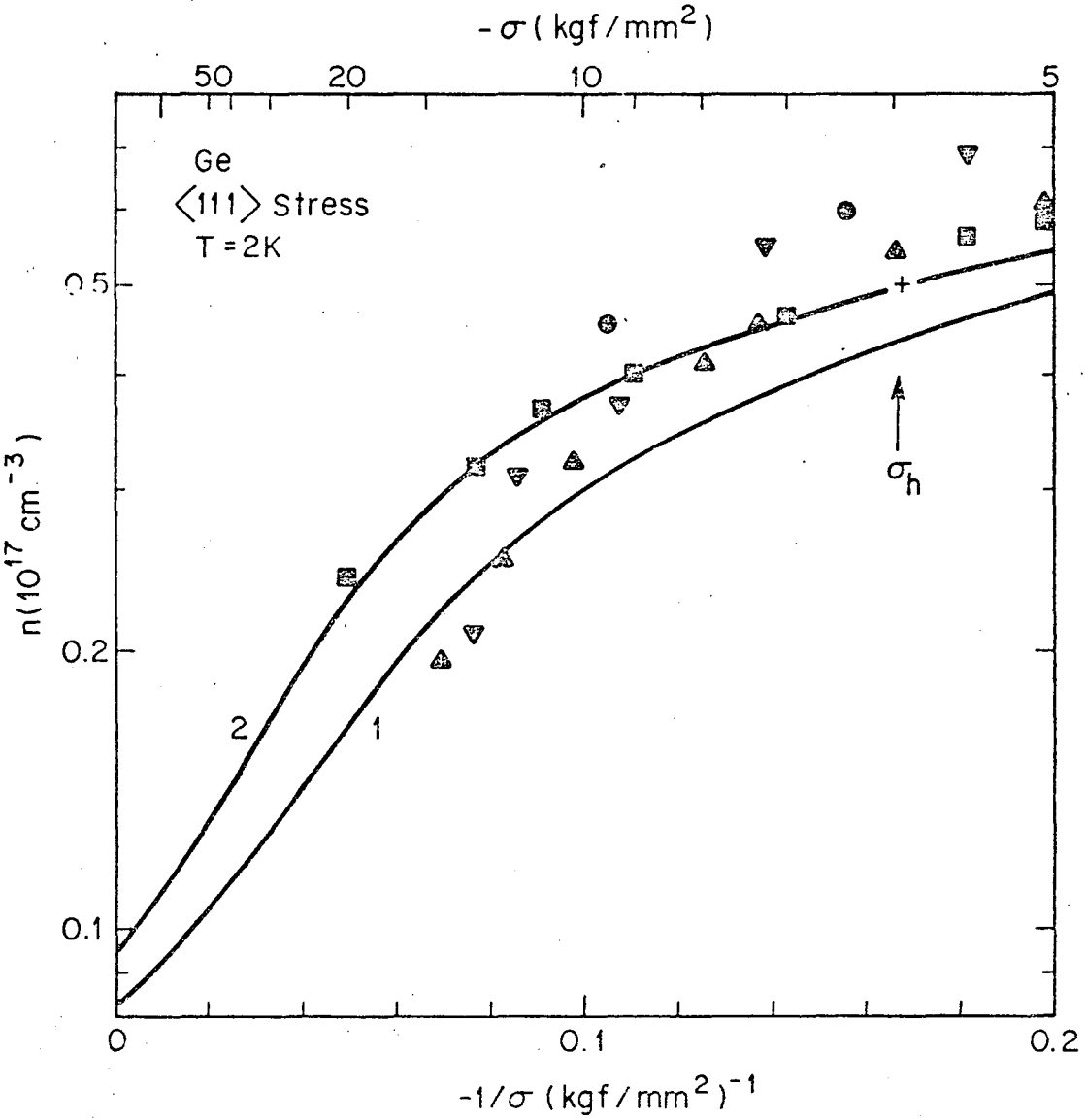
$-\sigma$ (kgf / mm^2)
50
20
10
5
Ge
⟨111⟩ Stress
T = 2K
0.5
0.2
0.1
n(10^{17} cm^{-3})
2
1
σ_h
0
0.1
0.2
$-1/\sigma$ (kgf / mm^2)$^{-1}$

FIG. 13

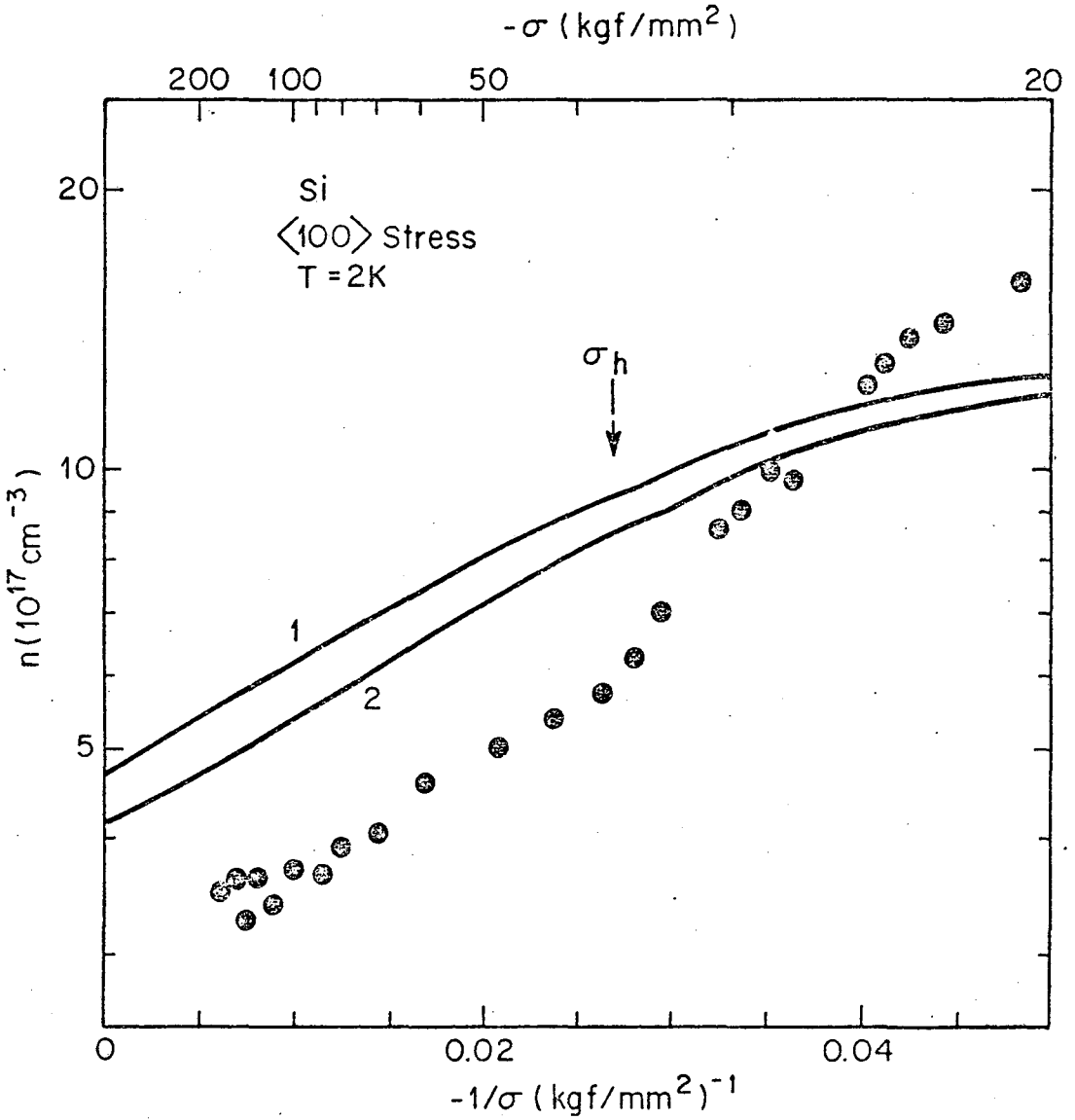
-σ (kgf/mm²)
200
100
50
20
Si
⟨100⟩ Stress
T = 2K
σh
1
2
20
10
5
n(10¹⁷cm⁻³)
0
0.02
0.04
-1/σ (kgf/mm²)⁻¹

FIG. 14

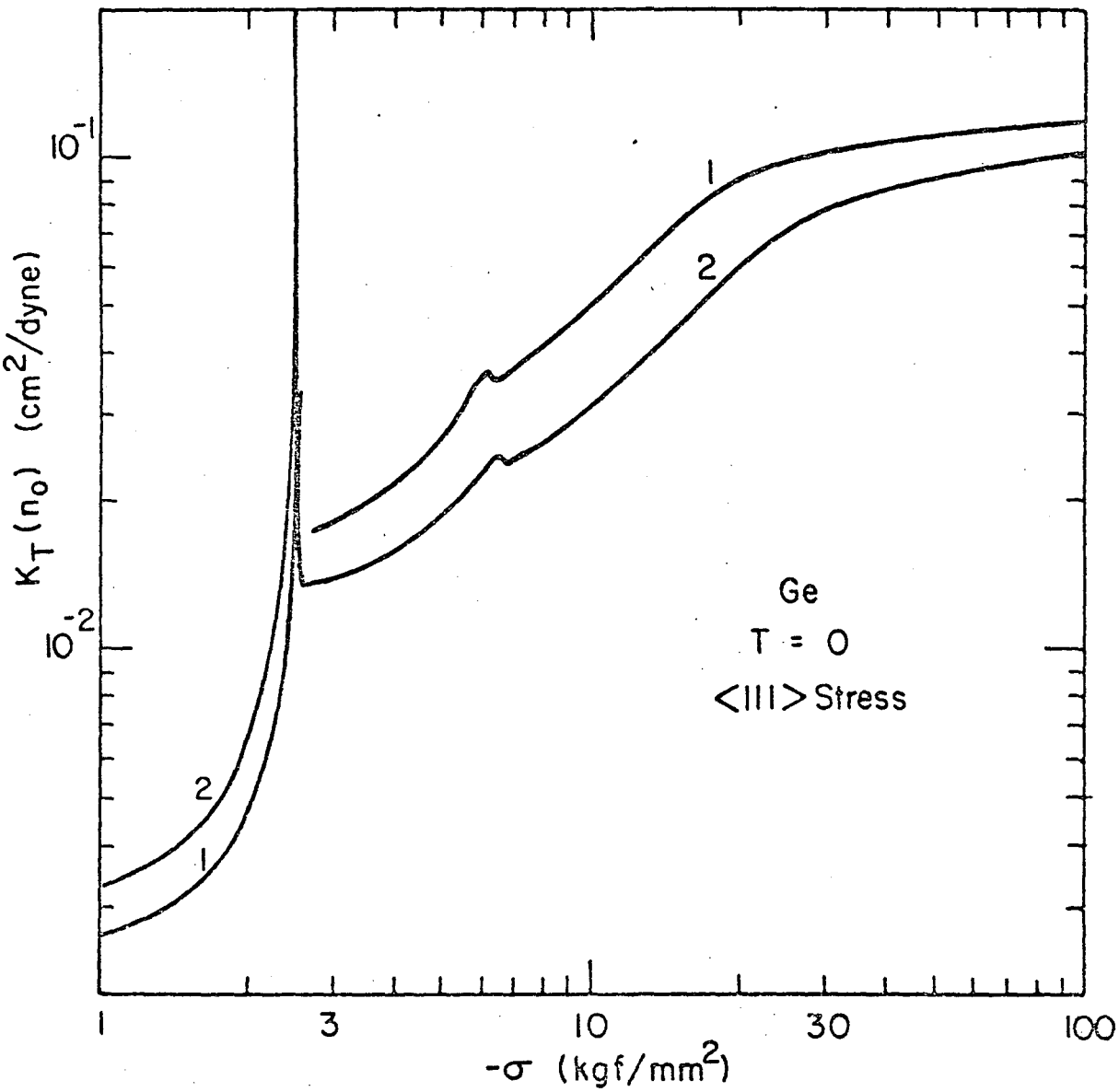
10^{-1}
10^{-2}
$K_T(n_o)$ (cm^2/dyne)
1
2
2
1
Ge
T = 0
<111> Stress
1
3
10
30
100
$-\sigma$ (kgf/mm^2)

FIG. 15

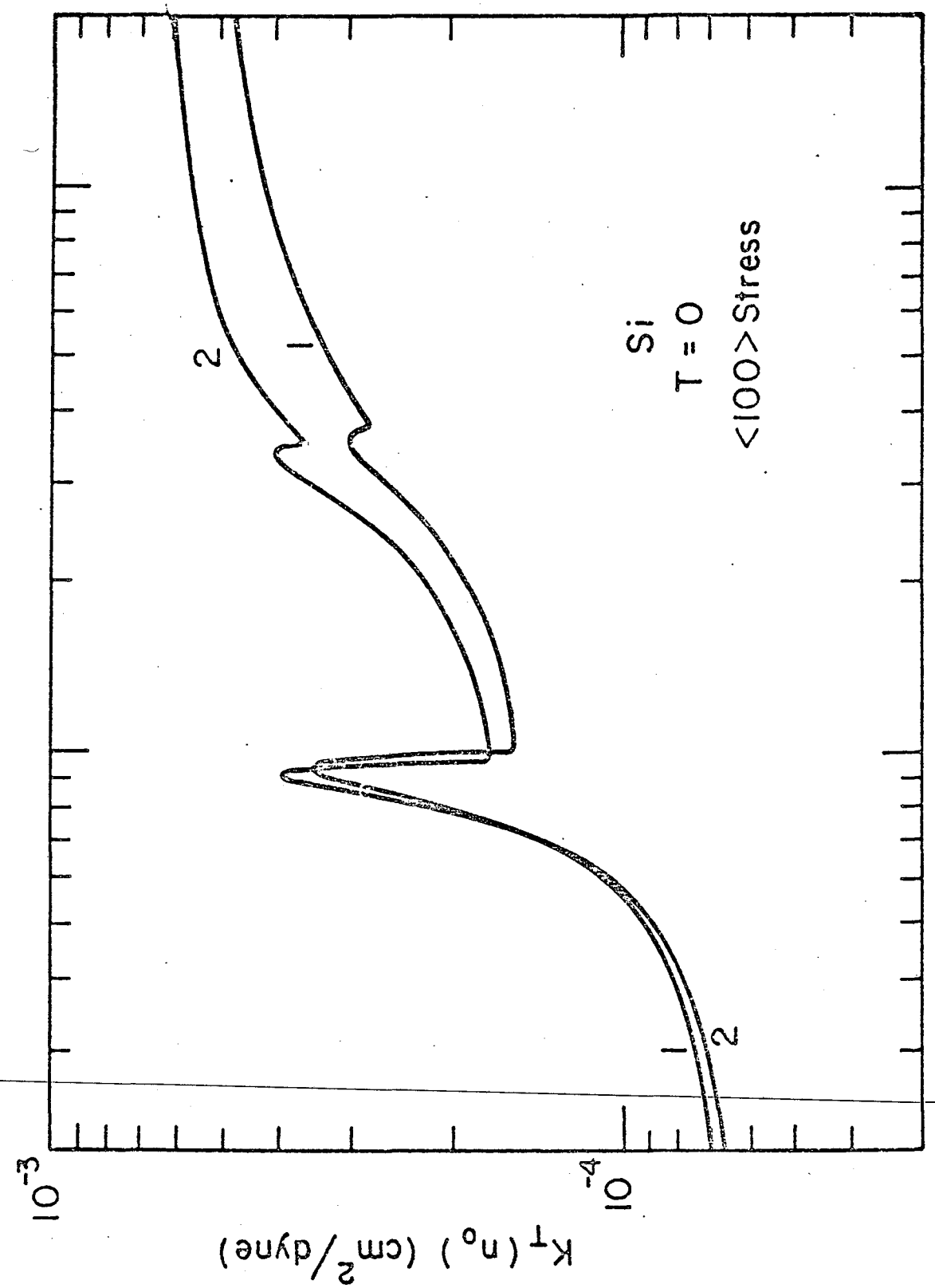
Si
T = 0
<100> Stress
2
1
1
2
10^{-3}
10^{-4}
3
10
30
100
$-\sigma$ (kgf/mm^2)
$K_T(n_o)$ (cm^2/dyne)

FIG. 16

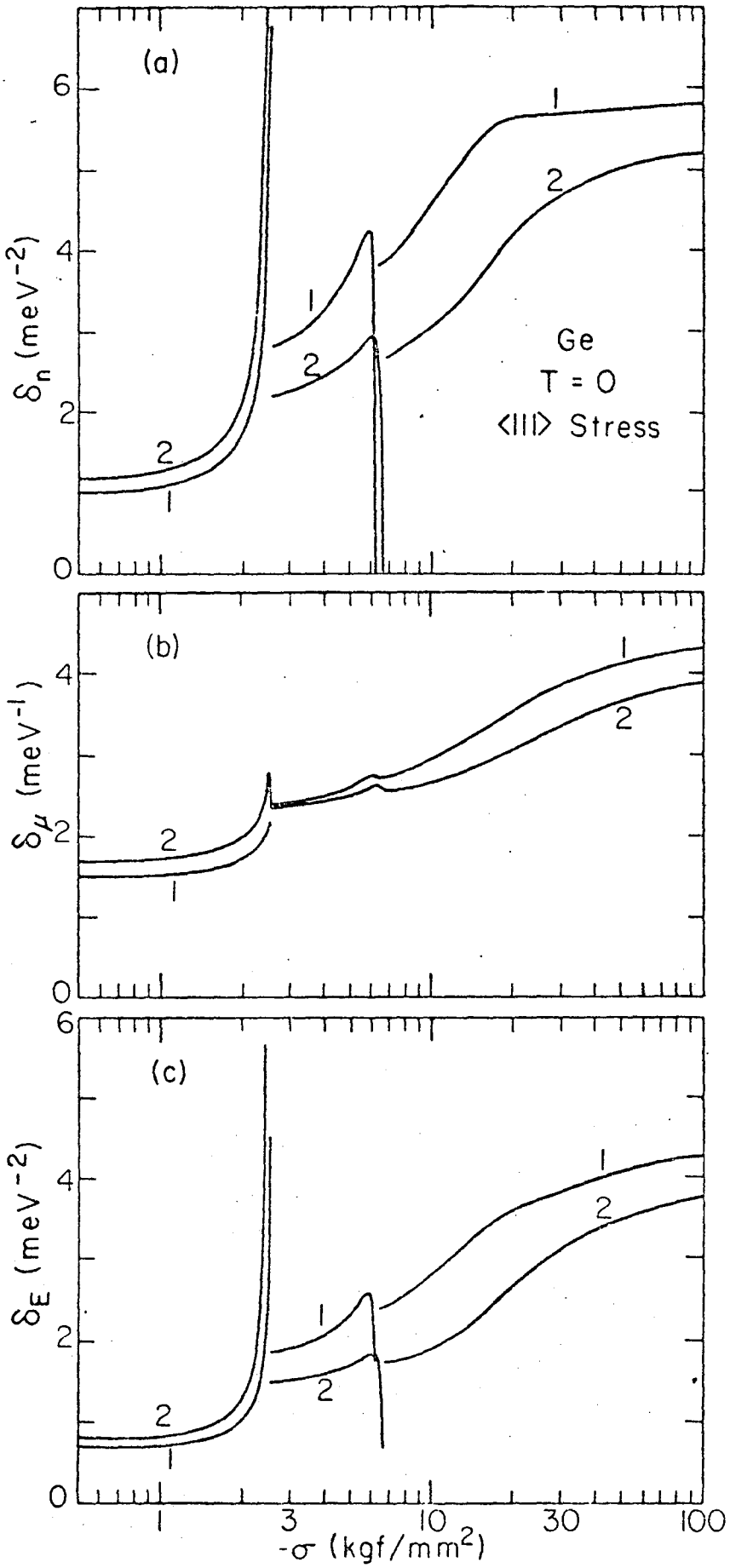
(a)
(b)
(c)
Ge
T = 0
⟨111⟩ Stress
δ_n (meV^{-2})
δ_μ (meV^{-1})
δ_E (meV^{-2})
-σ (kgf/mm^2)
0
2
4
6
1
3
10
30
100
1
2

FIG. 17

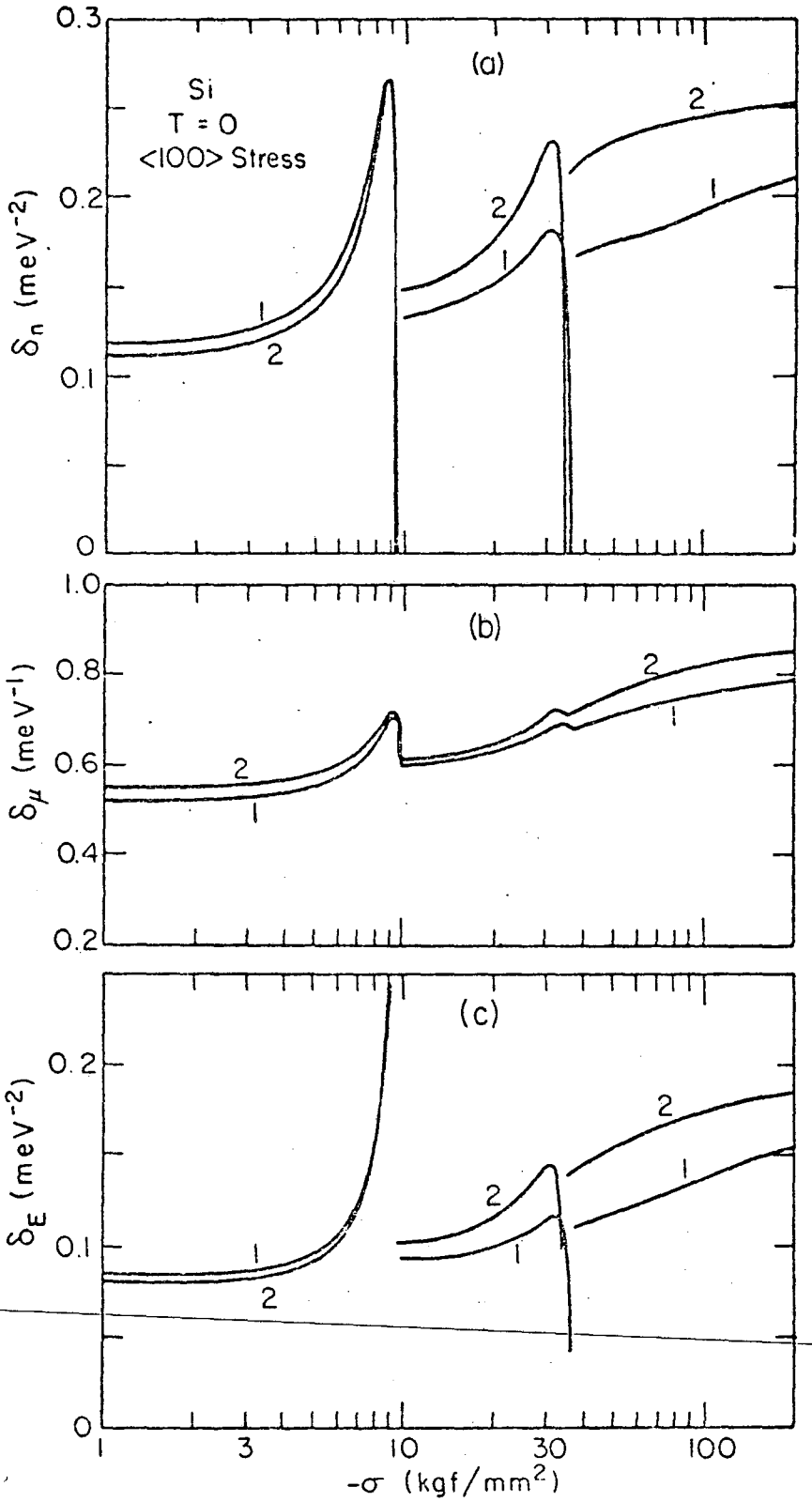
(a)
Si
T = 0
<100> Stress
δ_n (meV^{-2})
0.3
0.2
0.1
0
(b)
δ_μ (meV^{-1})
1.0
0.8
0.6
0.4
0.2
(c)
δ_E (meV^{-2})
0.2
0.1
0
1
2
3
10
30
100
$-\sigma$ (kgf/mm^2)

FIG. 18

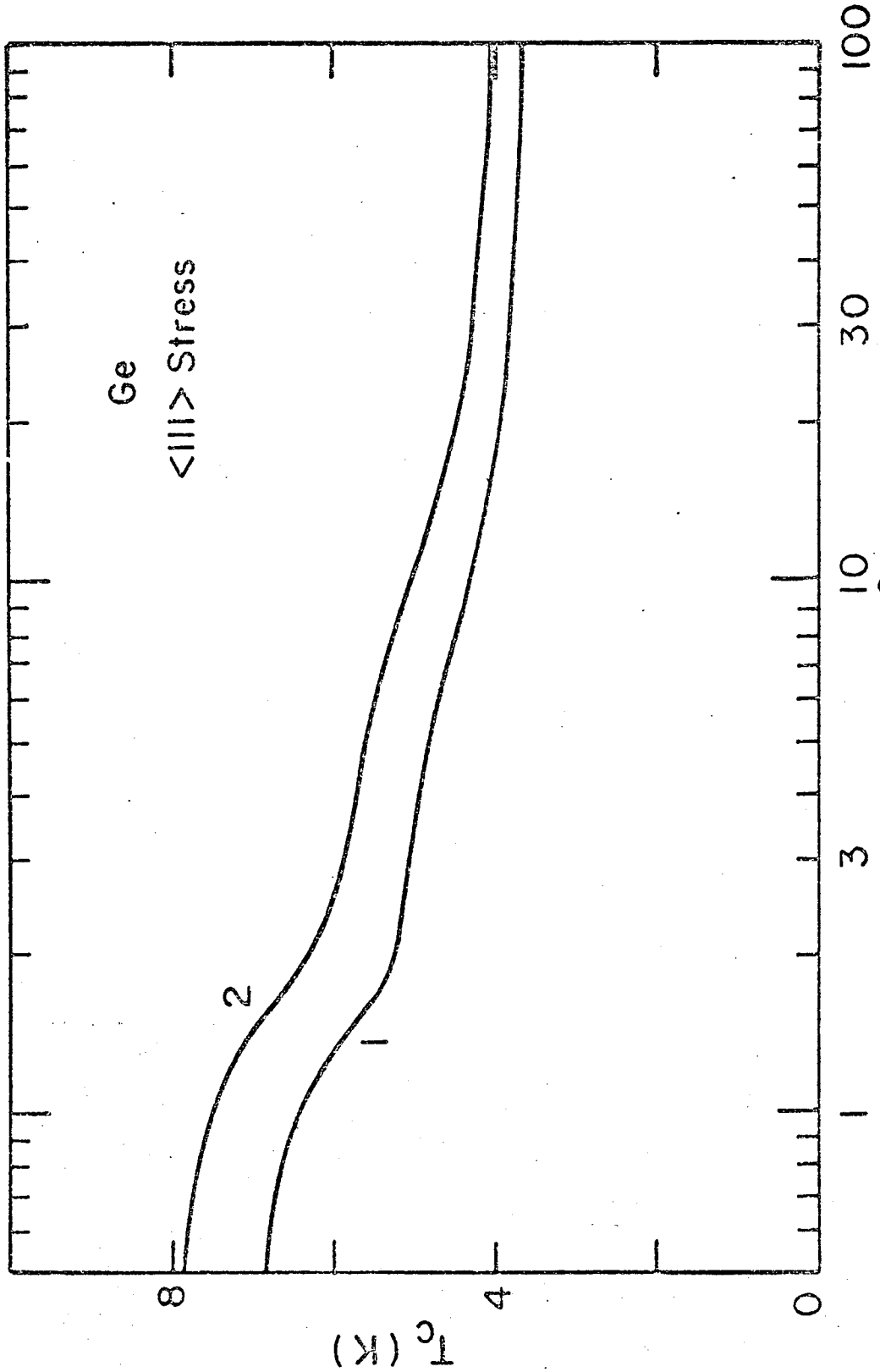

FIG. 19

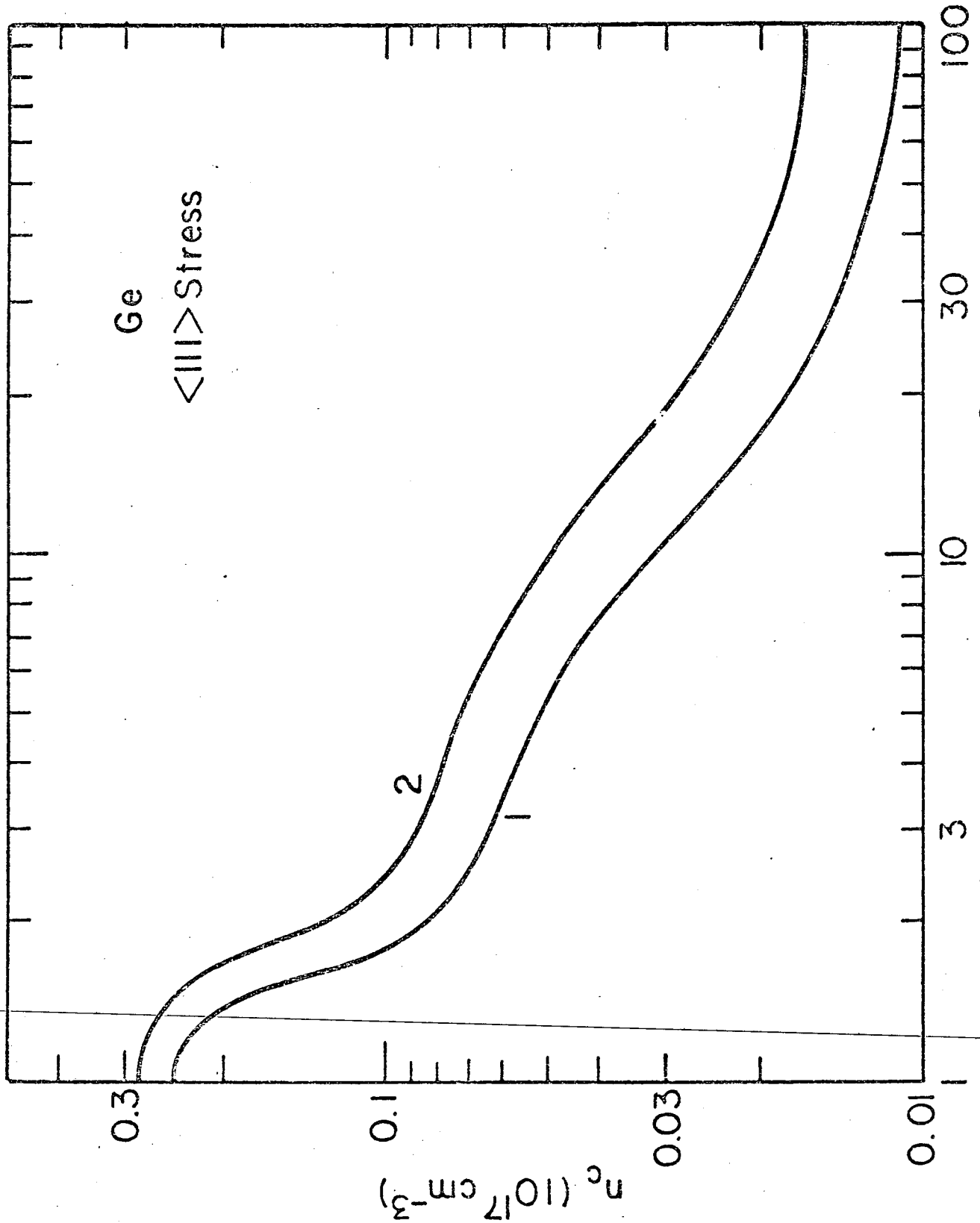
Ge
<111> Stress
2
1
0.3
0.1
0.03
0.01
3
10
30
100
n_c (10^{17} cm^{-3})
$-\sigma$ (kgf/mm^2)

FIG. 20

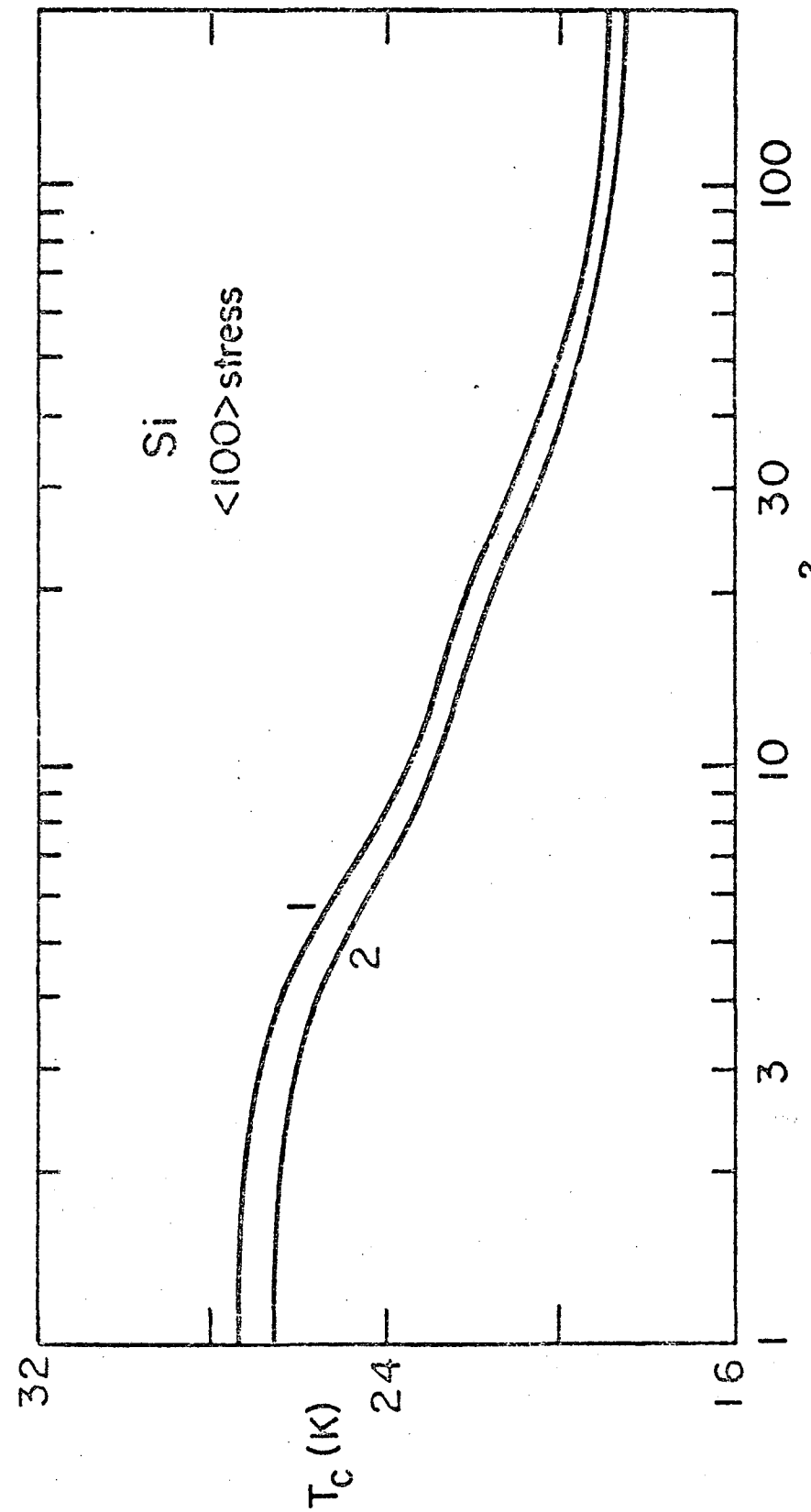

FIG. 21

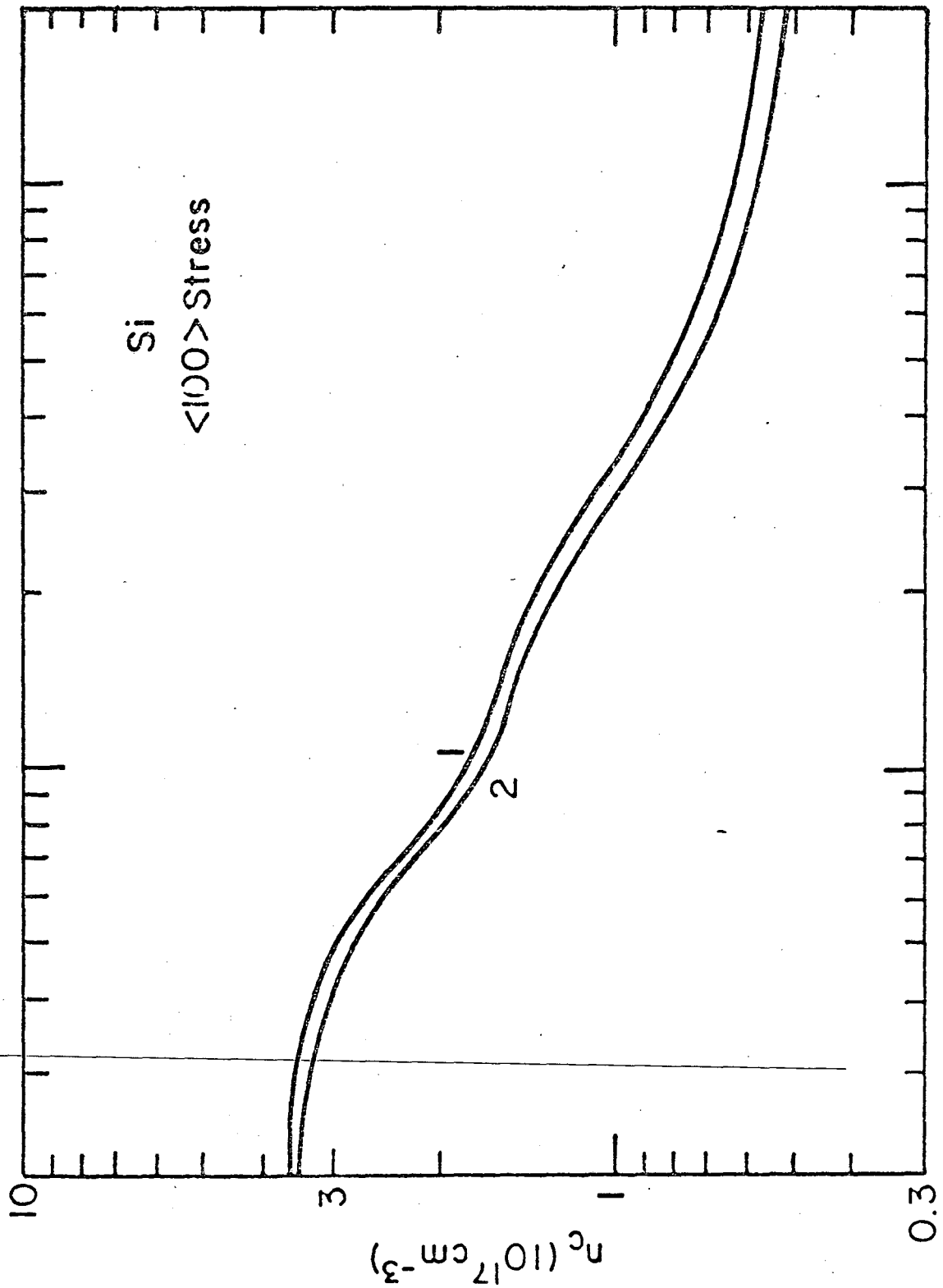

FIG. 22

This report was done with support from the Department of Energy. Any conclusions or opinions expressed in this report represent solely those of the author(s) and not necessarily those of The Regents of the University of California, the Lawrence Berkeley Laboratory or the Department of Energy.

Reference to a company or product name does not imply approval or recommendation of the product by the University of California or the U.S. Department of Energy to the exclusion of others that may be suitable.

TECHNICAL INFORMATION DEPARTMENT
LAWRENCE BERKELEY LABORATORY
UNIVERSITY OF CALIFORNIA
BERKELEY, CALIFORNIA 94720